Original Article

MOLECULAR METABOLISM

# Glucose inhibits glucagon secretion by decreasing $[Ca^{2+}]_c$ and by reducing the efficacy of $Ca^{2+}$ on exocytosis via somatostatin-dependent and independent mechanisms

**Bilal Singh, Firas Khattab, Patrick Gilon***

## ABSTRACT

**Objective:** The mechanisms by which glucose stimulates insulin secretion from β-cells are well established and involve inhibition of ATP-sensitive $K^+$ ($K_{ATP}$) channels, followed by a rise in $[Ca^{2+}]_c$ that triggers exocytosis. However, the mechanisms by which glucose controls glucagon release from α-cells are much less known. In particular, it is debated whether the sugar controls glucagon secretion by changing α-cell $[Ca^{2+}]_c$, and whether $K_{ATP}$ channels or paracrine factors are involved. The present study addresses these issues.

**Methods:** We tested the effect of a decrease or an increase of glucose concentration (Gx, with x = concentration in mM) on α-cell $[Ca^{2+}]_c$ and glucagon secretion. α-cell $[Ca^{2+}]_c$ was monitored using *GluCreGCaMP6f* mice expressing the $Ca^{2+}$-sensitive fluorescent protein, GCaMP6f, specifically in α-cells. $[Ca^{2+}]_c$ was compared between dispersed α-cells and α-cells within islets to evaluate the potential contribution of an indirect effect of glucose. The same protocols were used for experiments of glucagon secretion from whole islets and $[Ca^{2+}]_c$ measurements to test if changes in glucagon release mirror those in α-cell $[Ca^{2+}]_c$.

**Results:** Blockade of $K_{ATP}$ channels by sulfonylureas (tolbutamide 100 μM or gliclazide 25 μM) strongly increased $[Ca^{2+}]_c$ in both dispersed α-cells and α-cells within islets. By contrast, glucose had no effect on $[Ca^{2+}]_c$ in dispersed α-cells, whereas it affected it in α-cells within islets. The effect of glucose was however different in islets expressing (*Sst*$^{+/+}$) or not somatostatin (SST) (*Sst*$^{-/-}$). Decreasing glucose concentration from G7 to G1 modestly increased α-cell $[Ca^{2+}]_c$, but to a slightly larger extent in *Sst*$^{+/+}$ islets than in *Sst*$^{-/-}$ islets. This G1-induced $[Ca^{2+}]_c$ rise was also observed in the continuous presence of sulfonylureas in both *Sst*$^{+/+}$ and *Sst*$^{-/-}$ islets. Increasing glucose concentration from G7 to G20 did not affect α-cell $[Ca^{2+}]_c$ in *Sst*$^{+/+}$ islets which remained low, whereas it strongly increased it in *Sst*$^{-/-}$ islets. The observations that this increase was seen only in α-cells within islets but never in dispersed α-cells and that it was abrogated by the gap junction inhibitor, carbenoxolone, point to an indirect effect of G20 and suggest that, in *Sst*$^{-/-}$ islets, G20-stimulated β-cells entrain α-cells whereas, in *Sst*$^{+/+}$ islets, the concomitant release of SST keeps α-cell $[Ca^{2+}]_c$ at low levels. The $[Ca^{2+}]_c$ lowering effect of endogenous SST is also supported by the observation that SST receptor antagonists (SSTR2/3) increased $[Ca^{2+}]_c$ in α-cells from *Sst*$^{+/+}$ islets. All these $[Ca^{2+}]_c$ changes induced parallel changes in glucagon release. To test if glucose also controls glucagon release independently of $[Ca^{2+}]_c$ changes, additional experiments were performed in the continuous presence of 30 mM $K^+$ and the $K_{ATP}$ channel opener diazoxide (250 μM). In these conditions, α-cell $[Ca^{2+}]_c$ within islets was elevated and its steady-state level was unaffected by glucose. However, decreasing the glucose concentration from G7 to G1 stimulated glucagon release whereas increasing it from G1 to G15 inhibited it. These effects were also evident in *Sst*$^{-/-}$ islets, and opposite to those on insulin secretion.

**Conclusions:** We propose a model according to which glucose controls α-cell $[Ca^{2+}]_c$ and glucagon secretion through multiple mechanisms. Increasing the glucose concentration modestly decreases $[Ca^{2+}]_c$ in α-cells independently of their $K_{ATP}$ channels and partly via SST. The involvement of SST increases with the glucose concentration, and one major effect of SST is to keep α-cell $[Ca^{2+}]_c$ at low levels by counteracting the effect of an entrainment of α-cells by β-cells when β-cells become stimulated by glucose. All these $[Ca^{2+}]_c$ changes induce parallel changes in glucagon release. Glucose also decreases the efficacy of $Ca^{2+}$ on exocytosis by an attenuating pathway that is opposite to the well-established amplifying pathway controlling insulin release in β-cells.



**Keywords** Pancreatic islets; $K_{ATP}$ channels; $Ca^{2+}$; Glucagon; Somatostatin

Université Catholique de Louvain, Institut de Recherche Expérimentale et Clinique, Pôle d'Endocrinologie, Diabète et Nutrition, Brussels, Belgium

*Corresponding author. Pôle d'Endocrinologie, Diabète et Nutrition, Avenue Hippocrate 55, B1.55.06, B-1200, Brussels, Belgium. E-mail: patrick.gilon@uclouvain.be (P. Gilon).

*Abbreviations:* $[Ca^{2+}]_c$, free cytosolic $Ca^{2+}$ concentration; cAMP, cyclic adenosine monophosphate; CBX, carbenoxolone; Epac, exchange protein directly activated by cAMP; GIRK channels, G protein-gated inwardly rectifying $K^+$ channels; HG, high glucose concentration; $K_{ATP}$ channels, ATP-sensitive $K^+$ channels; LG, low glucose concentration; NG, NormoGlycemic range; SERCA, sarco/endoplasmic reticulum $Ca^{2+}$-ATPase; SST, somatostatin; SSTR, somatostatin receptor; VGCC, voltage-gated $Ca^{2+}$ channels

Received November 23, 2021 • Revision received March 15, 2022 • Accepted April 4, 2022 • Available online 11 April 2022

https://doi.org/10.1016/j.molmet.2022.101495

 

## 1. INTRODUCTION

Glucagon, released by pancreatic α-cells in response to hypoglycemia, plays a major role in glucose homeostasis by counteracting the action of insulin [1]. Its main effect is to mobilize glucose from the liver by promoting glycogenolysis and gluconeogenesis, but it also regulates amino acid metabolism by increasing ureagenesis [2,3]. Insulin, released by pancreatic β-cells in response to hyperglycemia, is the main hypoglycemic hormone [4]. Diabetes is a metabolic disease in which insulin secretion/action is impaired, leading to hyperglycemia. It is also characterized by hyperglucagonemia which aggravates hyperglycemia. Moreover, diabetic patients suffer from an impaired glucagon response to hypoglycemia, which can lead to potentially life-threatening hypoglycemic coma [5–7].

The mechanisms by which glucose stimulates insulin secretion are well established. By entering β-cells, glucose increases the ATP/ADP ratio which closes ATP-sensitive $K^+$ ($K_{ATP}$) channels in the plasma membrane. The resulting decrease in $K^+$ conductance depolarizes the plasma membrane to a potential which reaches the threshold for activation of high-threshold voltage-gated $Ca^{2+}$ channels (VGCC), mainly L-type, leading to their opening and the subsequent rise in the cytosolic free $Ca^{2+}$ concentration ($[Ca^{2+}]_c$), which triggers exocytosis [4,8]. Despite sharing key components of β-cells (such as $K_{ATP}$ channels and L-type VGCC), α-cells are not stimulated, but instead inhibited by glucose. It is well established that a rise in $[Ca^{2+}]_c$ in α-cells triggers exocytosis of glucagon [9]. However, it is still unclear whether the control of glucagon secretion by glucose requires changes in α-cell $[Ca^{2+}]_c$. Experiments on dispersed islet cells show very divergent results. An increase of glucose concentration decreased [10–12], increased [13], or did not clearly affect α-cell $[Ca^{2+}]_c$ [14–16]. Because these effects were observed on isolated cells, it is assumed that they result from a direct action of glucose on α-cells (intrinsic control). Several mechanisms of inhibition by glucose have been proposed [7,17–20]. The store-operated model suggests that an increase in the glucose concentration activates sarco-endoplasmic reticulum $Ca^{2+}$-ATPase (SERCA), which fills the endoplasmic reticulum (ER) with $Ca^{2+}$, leading to an inhibition of a depolarizing store-operated current, a reduction in the activity of VGCC and a decrease in $[Ca^{2+}]_c$ [17]. An alternative model suggests that the drop in $[Ca^{2+}]_c$ induced by glucose results from a closure of $K_{ATP}$ channels which depolarizes the cell and leads to an inactivation of low-threshold voltage-gated channels (mainly $Na^+$ ($Na_v$) and less importantly T-type $Ca^{2+}$ channels), a reduction in action potential amplitude and a decrease in $Ca^{2+}$ influx via VGCC (mostly P/Q type) [21–24]. This model is however difficult to reconcile with some studies reporting that $K_{ATP}$ channel blockers increase α-cell $[Ca^{2+}]_c$ [11,14,25–29]. Other models include the activation by glucose of the hyperpolarizing $Na^+/K^+$ pump [30] or of the two-pore-domain $K^+$ channel (K2P), TASK1 [31], or the inhibition by glucose of $Ca^{2+}$-activated $K^+$ channels that limits $Ca^{2+}$ influx [32]. These mechanisms are however in contradiction with the study by Olsen et al. [13] showing that glucose increases α-cell $[Ca^{2+}]_c$ by closing $K_{ATP}$ channels leading to a stimulation of $Ca^{2+}$ influx, as in β-cells. Experiments on whole islets also reported contradictory results [15,16,23,33–38]. Thus, $[Ca^{2+}]_c$ measurements in α-cells by confocal or total internal reflection fluorescence (TIRF) microscopy with chemical probes reported that glucose decreased [23,33,34,39], increased [16,36], or did not clearly affect α-cell $[Ca^{2+}]_c$ [15,16,36,37,39,40]. Heterogeneous and sometimes opposite responses were observed in subsets of α-cells within the same study [15,16,36–38,39,40]. $[Ca^{2+}]_c$ measurements with the $Ca^{2+}$-sensitive protein GCaMP3 targeted specifically to α-cells reported that glucose decreased $[Ca^{2+}]_c$ [35]. The control of $[Ca^{2+}]_c$ in α-cells within islets might involve mechanisms additional to those responsible for the intrinsic control [7,17–20]. They include a control by paracrine factors such as somatostatin (SST) released by δ-cells [41,42–44], juxtacrine signalling [40,45,46] or electrical coupling between cells [47]. The causes of all the discrepant effects of glucose on α-cell $[Ca^{2+}]_c$ are unclear and might be attributed to differences in experimental conditions, models or techniques. The cell specificity of $[Ca^{2+}]_c$ measurements is likely inferior with chemical $Ca^{2+}$ probes than with $Ca^{2+}$-sensitive proteins targeted to α-cells, even using optical sectioning tools. It has also been suggested that glucose induces a local decrease in $[Ca^{2+}]_c$ that would not be visible with whole cell imaging [15]. It is possible that the effects of glucose depend on the concentration used [38]. All these divergent results and different hypotheses illustrate the complexity of α-cell control by glucose, and probably reflects our poor understanding of this control.

In the present study, we used a transgenic mouse model expressing the $Ca^{2+}$ indicator, GCaMP6f, specifically in α-cells (*GluCreGCaMP6f/Sst*$^{+/+}$ mice) to study the mechanisms of control of α-cell $[Ca^{2+}]_c$ by glucose. We chose this probe because it has a better sensitivity, a higher performance and is more suitable for fast $Ca^{2+}$ dynamics than GCaMP3 [48–50]. We compared the $[Ca^{2+}]_c$ responses in dispersed α-cells *versus* α-cells within islets. We evaluated the role of $K_{ATP}$ channels in the effect of glucose using sulfonylureas which close these channels. To investigate the involvement of SST, we crossed *GluCreGCaMP6f/Sst*$^{+/+}$ mice with *Sst*$^{-/-}$ mice to generate *GluCreGCaMP6f/Sst*$^{-/-}$ and used antagonists of SST receptors (SSTR). Since we previously reported that the dose–response curve of the effect of glucose on glucagon secretion displays a U-shape in *Sst*$^{-/-}$ mice (but not in *Sst*$^{+/+}$ mice), with a minimum at 7 mM glucose [43], we tested the effect of a change in the glucose concentration in two opposite directions: a drop from 7 mM (referred to as NG for NormoGlycemic range) to 1 mM (LG: Low Glucose), and a rise from 7 mM to 15–20 mM (HG: High Glucose). By measuring $[Ca^{2+}]_c$ changes in α-cells within islets and glucagon secretion using the same perifusion protocols, we tested whether the changes in glucagon secretion mirror those in $[Ca^{2+}]_c$. We report that glucose acts via several pathways to inhibit glucagon secretion, depending on the glucose concentration. Decreasing the glucose concentration from NG to LG increases α-cell $[Ca^{2+}]_c$ and stimulates glucagon release by a mechanism that is independent of $K_{ATP}$ channels and, at least partly, independent of SST. On the other hand, increasing the glucose concentration from NG to HG increases α-cell $[Ca^{2+}]_c$ and glucagon secretion in *Sst*$^{-/-}$ islets but not in *Sst*$^{+/+}$ islets, which indicates that, in *Sst*$^{+/+}$ islets, HG starts to recruit SST to inhibit $[Ca^{2+}]_c$ and glucagon release. The stimulatory effect of HG in the absence of SST is indirect because it is lost in dispersed α-cells. We also demonstrate that LG increases the efficacy of $Ca^{2+}$ on exocytosis in α-cells while HG decreases it by SST-independent mechanisms.

## 2. MATERIALS AND METHODS

### 2.1. Animals

Two mouse models were used, *GluCreGCaMP6f/Sst*$^{+/+}$ and *GluCreGCaMP6f/Sst*$^{-/-}$ mice, as previously described [29]. The first model was generated by crossing *Lox-STOP-Lox-GCaMP6f/Sst*$^{+/+}$ mice *(obtained from Jackson Laboratory* stock No: 024105) with *GluCre/Sst*$^{+/+}$ mice, previously described [51]. This crossing allows the excision of the STOP cassette and the subsequent expression of GCaMP6f specifically in α-cells. *GluCreGCaMP6f/Sst*$^{-/-}$ mice were generated by further crossing *GluCreGCaMP6f/Sst*$^{+/+}$ mice with *Sst*$^{-/-}$ mice [52]. This

 

model is thus characterized by the expression of GCaMP6f specifically in α-cells and the lack of expression of SST. The study was approved by our ethics commission for animal experimentation (2014/UCL/MD/016 and 2018/UCL/MD/18 projects).

### 2.2. Solutions and drugs

The medium used for perifusion and $[Ca^{2+}]_c$ experiments contained (in mM) 124 NaCl, 4.8 KCl, 2.5 $CaCl_2$, 1.2 $MgCl_2$, 20 $NaHCO_3$ and 1 mg/ml BSA, and was supplemented with a mixture of 6 mM amino acids (2 mM alanine, 2 mM arginine and 2 mM glutamine). In experiments with K30, NaCl and KCl concentrations were 98.8 mM and 30 mM, respectively, to maintain the osmolarity of the medium constant. The medium had a pH of 7.4 and was continuously gassed throughout the experiments with $O_2$:$CO_2$ (95:5%). Test agents were added as indicated in the figures except for thapsigargin (2 μM) which was added in preincubation for 2 h. Adrenaline was obtained from Sterop, CYN154806 from Tocris, collagenase P from Roche, H6056 from Bachem and RO280450 from Axon Medchem. All other compounds were obtained from Merck.

### 2.3. Preparation of isolated islets and dispersed cells

Pancreases from *GluCreGCaMP6f/Sst*$^{+/+}$ and *GluCreGCaMP6f/Sst*$^{-/-}$ mice were digested with collagenase P (0.65 mg/ml) to obtain isolated islets. Dispersed cells were plated on coverslips after dissociating isolated islets with trypsin—EDTA (0.25%). Isolated islets for perifusion experiments were cultured overnight in RPMI 1640 medium containing 7 mM glucose and 10% heat inactivated FBS whereas isolated islets and dispersed cells for $[Ca^{2+}]_c$ experiments were cultured for up to 3 days.

### 2.4. Dynamic secretion experiments with isolated islets

Isolated islets (150—250) were placed in 750 μl chambers and perifused at 37 °C at a flow rate of 0.5 ml/min. After a 20 min equilibration period with the first solution, effluent was collected every 2.5 min. Glucagon (Merck Millipore GL-32 K) and insulin (homemade assay) were measured by radioimmunoassay. We verified that all drugs did not interfere with the assays.

### 2.5. $[Ca^{2+}]_c$ measurements

Isolated islets and dispersed cells were placed in 1.5 ml chambers and perifused at 37 °C at a flow rate of 0.5 ml/min. A Zeiss Axiovert 100 inverted microscope equipped with a 40x objective was used to measure changes in GCaMP6f fluorescence in dispersed α-cells. A Nikon eclipse TE2000-E inverted microscope equipped with a 40x objective and a confocal QLC100 spinning disk was used to measure changes in GCaMP6f fluorescence in α-cells within islets. GCaMP6f was excited at 491 nm (confocal) or 495 nm (epifluorescence) and emitted fluorescence was recorded at 503—552 nm (confocal) or 510—560 (epifluorescence). An EMCCD QuantEM 512SC or a sCMOS Prime 95 B (Photometrics) camera controlled by Metafluor software was used to acquire the images every 1—3 s.

We previously assessed the α-cell specificity of GCaMP6f expression [29]. It was very high: 96% in *GluCreGCaMP6f/Sst*$^{+/+}$ mice and 94% in *GluCreGCaMP6f/Sst*$^{-/-}$ mice. To further ensure the identity of α-cells analyzed in this study, we systematically applied adrenaline, an α-cell specific secretagogue [10], at the end of all $[Ca^{2+}]_c$ experiments. Only cells responding to adrenaline by a rise in $[Ca^{2+}]_c$ were considered as α-cells and selected (representative traces shown in Supplementary Figures).

### 2.6. Statistical analyses and data presentation

Results are presented as representative traces or means ± SEM for islets or dispersed cells from at least three different mice (n = number of cells for $[Ca^{2+}]_c$ experiments or number of islet preparations from different mice for secretion experiments). Secretion experiments are presented as pg/islet/min whereas $[Ca^{2+}]_c$ measurements are presented as $F/F_0$ where F is the fluorescence intensity at a given time point and $F_0$ the lowest fluorescence intensity. Because of the lack of synchronicity of $[Ca^{2+}]_c$ changes between α-cells within and between experiments, the times at which the minimum ($F/F_0 = 1$) occur are different between cells. This explains why the mean of the $F/F_0$ is always higher than 1. Two-tailed paired Student t-test was used for two sample comparisons of the same cell or islet batch whereas two-tailed unpaired Student t-test was used to compare two different populations of cells or batches of islets. Ordinary two-way, one-way or two-way RM ANOVA with post hoc Sidak correction was used for multiple comparisons. In most experiments in which an agent was tested acutely and with a reversibility period, the comparison was performed between the average of the period with the test agent and the average of the periods preceding and following the test agent (times indicated in the legends of the figures). This corrected for the bias resulting from the spontaneous decrease or increase of the measured signal ($[Ca^{2+}]_c$ or secretion) over time. All statistical tests were calculated using GraphPad Prism 8.

## 3. RESULTS

### 3.1. Decreasing the glucose concentration from NG to LG increases α-cell $[Ca^{2+}]_c$ and stimulates glucagon secretion by SST-dependent and independent mechanisms

Using the *GluCreGCaMP6f/Sst*$^{+/+}$ mouse model, we evaluated the effect of a decrease of the glucose concentration from NG to LG on α-cell $[Ca^{2+}]_c$. Switching from 7 mM (G7) to 1 mM glucose (G1) had no consistent effect on $[Ca^{2+}]_c$ in dispersed α-cells (Figure 1A,B and Supplementary Figure S1A). Only 3 cells out of 15 (20%) responded with an increase in $[Ca^{2+}]_c$ (with, at least, a 5% increase in fluorescence intensity between 17 and 25 min *versus* 2—10 and 32—40 min) while others did not respond (5/15) or responded with a decrease (7/15) (Figure 1F). Since the $F/F_0$ signal spontaneously decreased over time by 10% on average (comparing mean of 17—25 min *versus* mean of 2—10 and 32—40 min) (see Figure 1A), we considered that only cells which displayed a decrease of >10% as being really inhibited by G1, which occurred in 4 out of 15 α-cells (26.7%). We then measured α-cell $[Ca^{2+}]_c$ within islets using a similar experimental protocol. Interestingly, the $Ca^{2+}$ activity was higher in α-cells within islets than in dispersed α-cells as shown by the more frequent $[Ca^{2+}]_c$ oscillations (compare Supplementary Figure S1A with Supplementary Figure S1B and C). The $[Ca^{2+}]_c$ response to G1 displayed again a high variability (Supplementary Figure S1B). However, imaging 935 α-cells within islets revealed that G1 significantly increased average $[Ca^{2+}]_c$ (Figure 1C,D: blue trace and triangles). This increase reflected a $[Ca^{2+}]_c$ rise in 43.7% of α-cells (409/935 α-cells with, at least, a 5% increase in fluorescence intensity between 17 and 23 min versus 2—8 min; Figure 1G: left histogram). 32.5% (304/935) of α-cells did not respond to G1 and 23.8% (222/935) responded with a decrease. Since the $F/F_0$ signal also spontaneously decreased over time (a 15% decrease estimated by extrapolation of the baseline in G7), we considered that only cells which displayed a decrease >15% (between 17-23 min and 2—8 min) as being really inhibited by G1, which occurred in a negligible fraction of α-cells (2.5%). It is unlikely that these cells were β-cells because they were still active in G1 and they responded to adrenaline that was systematically applied at the end of the experiments (not shown). The observation that G1 increased average $[Ca^{2+}]_c$ in α-cells within islets but had no significant effect in

 

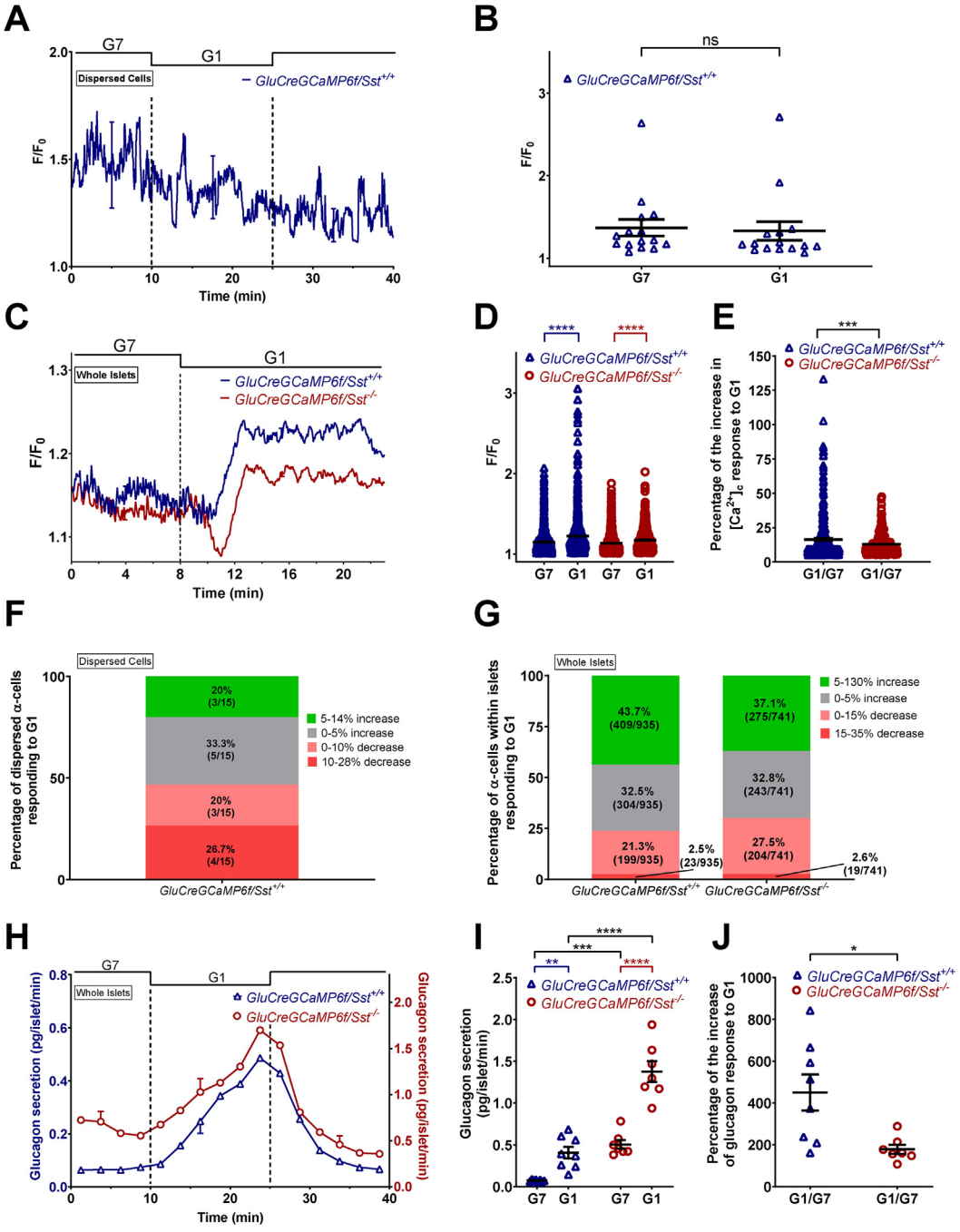


**Figure 1: Low glucose concentration stimulates glucagon secretion and elevates $[Ca^{2+}]_c$ in a small percentage of α-cells within islets.** α-cell $[Ca^{2+}]_c$ (A–E) was measured in either dispersed cells (A and B) or whole islets (C–E) from either *GluCreGCaMP6f/Sst*$^{+/+}$ (blue traces) or *GluCreGCaMP6f/Sst*$^{-/-}$ (red traces) mice. Glucagon secretion was measured in whole islets from either *GluCreGCaMP6f/Sst*$^{+/+}$ (blue trace) or *GluCreGCaMP6f/Sst*$^{-/-}$ (red trace) (H–J). Dispersed cells or whole islets were perifused consecutively with 7 mM (G7) and 1 mM glucose (G1). Panel A represents the mean traces ± SEM of 15 cells from 3 experiments. Panel C represents the mean traces ± SEM of 935 cells from 64 experiments (blue trace) and 741 cells from 58 experiments (red trace). Panel H represents the mean traces ± SEM of 8 (blue trace) and 7 experiments (red trace). Panels B and D represent the scatter plots of individual cells (B, n = 15 cells/3 mice; D, n = 935 cells/107 islets/27 *GluCreGCaMP6f/Sst*$^{+/+}$ mice and n = 741 cells/104 islets/18 *GluCreGCaMP6f/Sst*$^{-/-}$ mice; two-tailed paired t-tests) with the means ± SEM of the average $[Ca^{2+}]_c$ calculated from panel A (G7, mean of 2–10 min and 32–40 min; G1, mean of 17–25 min) and C (G7, mean of 2–8 min; G1, mean of 17–23 min), respectively. Panels F and G represent stacked columns showing the percentage of dispersed α-cells (F) and α-cells within islets (G) responding to G1 with a decrease (light red and red) and an increase (green) in $[Ca^{2+}]_c$ and the percentage of α-cells which do not respond to G1 (grey), based on the ratio of the signal from Figure 1A (mean of 17–25 min/mean of 2–10 min and 32–40 min; F) and Figure 1C (mean of 2–8 min/mean of 17–23 min; G). Panel I represents the scatter plot of individual experiments with the means ± SEM (Ordinary two-way and two-way RM ANOVA with Sidak correction) of the average glucagon secretion calculated from panel H (G7, mean of 2–10 min and 32–40 min; G1, mean of 17–25 min). Panels E and J represent the scatter plots showing the percentage of the increase in $[Ca^{2+}]_c$ (mean of 2–8 min/mean of 17–23 min) or glucagon (mean of 17–25 min/mean of 2–10 min and 32–40 min) in response to G1 (two-tailed unpaired t-tests), calculated from panels C and H, respectively. ns, not significant; *P < 0.05; **P < 0.005; ***P < 0.001; ****P < 0.0001.

 

isolated α-cells (compare Figure 1A with 1C) suggests that intra-islet factors modulate α-cell activity. Such factors might involve contact-dependent signalling (including juxtacrine influence and electrical coupling), or paracrine/autocrine factors. Since SST acts as a strong paracrine regulator of α-cells, we suspected SST to be involved. Therefore, we performed the same experiment using *GluCreGCaMP6f/Sst*$^{-/-}$ islets. Imaging 741 α-cells revealed that G1 significantly increased average $[Ca^{2+}]_c$ (Figure 1C,D: red trace and circles, and Supplementary Figure S1C). However, the amplitude of the increase (12.8% increase) was lower than in α-cells from *GluCreGCaMP6f/Sst*$^{+/+}$ islets (16.3% increase) (Figure 1E), probably because a lower percentage of α-cells (37.1%) responded to G1 with a $[Ca^{2+}]_c$ increase (275/741 α-cells with, at least, a 5% increase in fluorescence intensity between 17 and 23 min versus 2—8 min) (Figure 1G: right histogram). Dynamic secretion experiments using a similar protocol showed that G1 strongly stimulated glucagon release of both *GluCreGCaMP6f/Sst*$^{+/+}$ and *GluCreGCaMP6f/Sst*$^{-/-}$ islets, with basal and stimulated glucagon secretions being higher in *Sst*$^{-/-}$ islets than in *Sst*$^{+/+}$ islets (Figure 1H,I: compare red and blue traces). This indicates that SST exerts a tonic inhibition on glucagon release. Furthermore, the amplitude of the increase of glucagon secretion in response to G1 was higher in *Sst*$^{+/+}$ islets (450%) than in *Sst*$^{-/-}$ islets (179%) (Figure 1J) and thus, at least partly, mirrored the higher increase in $[Ca^{2+}]_c$.

The observation that the rise in α-cell $[Ca^{2+}]_c$ induced by G1 was significantly larger in *Sst*$^{+/+}$ than in *Sst*$^{-/-}$ islets (Figure 1E) suggests that the associated drop in SST secretion of *Sst*$^{+/+}$ islets contributes to the $[Ca^{2+}]_c$ rise. To further evaluate this hypothesis, we tested the effect of exogenous SST-14 on α-cell $[Ca^{2+}]_c$ of *Sst*$^{+/+}$ islets in G1 and G7 (Figure 2A—C). Interestingly, the amplitude of the SST-induced drop in $[Ca^{2+}]_c$ was much smaller in G7 than in G1 probably because endogenous SST released in response to G7 had already decreased $[Ca^{2+}]_c$ (Figure 2C).

To verify the role of SST in the control of glucagon secretion by glucose, we applied G1 in the presence of somatostatin receptor (SSTR) antagonists. The acute application of the antagonists also allows to test the effect of endogenous SST on $[Ca^{2+}]_c$ and glucagon release. Since α-cells mainly express SSTR2 and SSTR3 [43], we used a combination of CYN154806 (300 nM), a SSTR2 antagonist, and H6056 (1 μM), a SSTR2/3 antagonist. Changing the glucose concentration from 7 to 1 mM slightly increased α-cell $[Ca^{2+}]_c$ but strongly stimulated glucagon secretion of *GluCreGCaMP6f/Sst*$^{+/+}$ islets and these effects were reversible (Figure 2D,G: blue traces). Subsequent application of the SSTR2/3 antagonists in a medium containing G7 elevated α-cell $[Ca^{2+}]_c$ and stimulated glucagon secretion, which supports an inhibitory effect of endogenous SST on $[Ca^{2+}]_c$ and glucagon release. Moreover, switching from G7 to G1 in the presence of these antagonists slightly increased α-cell $[Ca^{2+}]_c$ and strongly stimulated glucagon secretion (Figure 2D,E, G and H: blue traces and triangles), also supporting the existence of a control of α-cell $[Ca^{2+}]_c$ and glucagon release by G1 that is independent of endogenous SST. Similar experiments were performed in *GluCreGCaMP6f/Sst*$^{-/-}$ islets. G1 increased α-cell $[Ca^{2+}]_c$ and stimulated glucagon secretion (Figure 2D,G: red traces). Surprisingly, the combination of both antagonists also slightly elevated α-cell $[Ca^{2+}]_c$ of *Sst*$^{-/-}$ mice while having no effect on glucagon secretion, probably because the effect on $[Ca^{2+}]_c$ was too small to affect glucagon secretion. The amplitude of the α-cell $[Ca^{2+}]_c$ increase was however smaller than that in Sst$^{+/+}$ islets (Figure 2F) supporting an inhibitory effect of endogenous SST on $[Ca^{2+}]_c$. Switching from G7 to G1 in the presence of the antagonists still increased α-cell $[Ca^{2+}]_c$ and glucagon secretion in this model lacking SST (Figure 2D,E, G and H: red traces and circles). Taken together, these data suggest that G1 induces an increase in α-cell $[Ca^{2+}]_c$ that is, for one part, dependent of endogenous SST, and, for another part, independent of SST. This $[Ca^{2+}]_c$ increase likely contributes to the glucagonotropic effect of G1. It is, however, of much smaller amplitude than that elicited by K30 (shown later in Figures 6A and 7A).

### 3.2. Decreasing the glucose concentration from NG to LG increases α-cell $[Ca^{2+}]_c$ and stimulates glucagon secretion independently of α-cell $K_{ATP}$ channels

We next investigated the role of $K_{ATP}$ channels in the control of α-cell $[Ca^{2+}]_c$ and glucagon secretion by glucose. Therefore, we tested the effect of glucose in the presence of a high concentration of the $K_{ATP}$ channel blocker, tolbutamide. Addition of 100 μM tolbutamide to a medium containing G7 increased $[Ca^{2+}]_c$ of both dispersed α-cells and α-cells within islets, and stimulated glucagon secretion from islets (Figure 3A—F and Supplementary Figure S2A and B). Switching from G7 to G1 further stimulated glucagon secretion with mild effect on $[Ca^{2+}]_c$ in α-cells within islets and no significant effect on $[Ca^{2+}]_c$ in dispersed α-cells. Readmission of G7 induced a decrease in $[Ca^{2+}]_c$ which was only transient in dispersed α-cells. Since it has been reported that tolbutamide could also act via a mechanism independent of $K_{ATP}$ channels, but dependant on Epac2 (exchange protein directly activated by cAMP 2), we repeated the same experiments using gliclazide, a $K_{ATP}$ channel blocker that lacks effect on Epac2 [53], and obtained similar results. 25 μM gliclazide increased α-cell $[Ca^{2+}]_c$ and stimulated glucagon release (Supplementary Figures S2C, D and S3). G1 in the presence of gliclazide also stimulated glucagon secretion with a slight increase in $[Ca^{2+}]_c$ in α-cells within islets. These data suggest that LG increases $[Ca^{2+}]_c$ and stimulates glucagon secretion independently of $K_{ATP}$ channels. We also performed similar experiments with *GluCreGCaMP6f/Sst*$^{-/-}$ islets which lack paracrine influence of SST. Tolbutamide increased α-cell $[Ca^{2+}]_c$ within islets and glucagon secretion in G7. Switching to G1 still slightly elevated $[Ca^{2+}]_c$ in α-cells but did not seem to stimulate glucagon secretion (Figure 3G—J and Supplementary Figure S4). However, switching back to G7 clearly inhibited glucagon secretion (Figure 3I), suggesting that G1 is stimulatory compared to G7. To test whether this stimulatory effect of G1 could be repeatedly observed, we performed an additional series of experiments in which we challenged the islets with two consecutive applications of G1 (Figure 3K and L). Switching twice from G7 to G1 clearly stimulated glucagon secretion in the presence of tolbutamide, and this effect was fully reversed when returning to G7, in islets expressing or not SST. This suggests that glucose controls glucagon secretion independently of $K_{ATP}$ channels and SST. Again, basal and stimulated glucagon secretions were higher in *Sst*$^{-/-}$ islets than in *Sst*$^{+/+}$ ones, reinforcing the conclusion that SST tonically inhibits glucagon secretion (Figure 3K and L).

### 3.3. In the absence of paracrine influence of SST, HG increases $[Ca^{2+}]_c$ in α-cells within islets and stimulates glucagon secretion by an indirect mechanism

We then evaluated the effect of an increase of glucose concentration from NG to HG on α-cell $[Ca^{2+}]_c$. In preparations from *GluCreGCaMP6f/Sst*$^{+/+}$ mice, switching from G7 to 20 mM glucose (G20) did not affect $[Ca^{2+}]_c$ in dispersed α-cells (Figure 4A,B: blue trace and triangles, and Supplementary Figure S5A), and it induced only a transient increase in α-cells within islets (Figure 4C,D: blue trace and triangles, and Supplementary Figure S5C). The amplitude of this transient $[Ca^{2+}]_c$ increase was variable between experiments and sometimes very small (Figure 5I, blue trace). Despite this transient increase, G20 had no

 

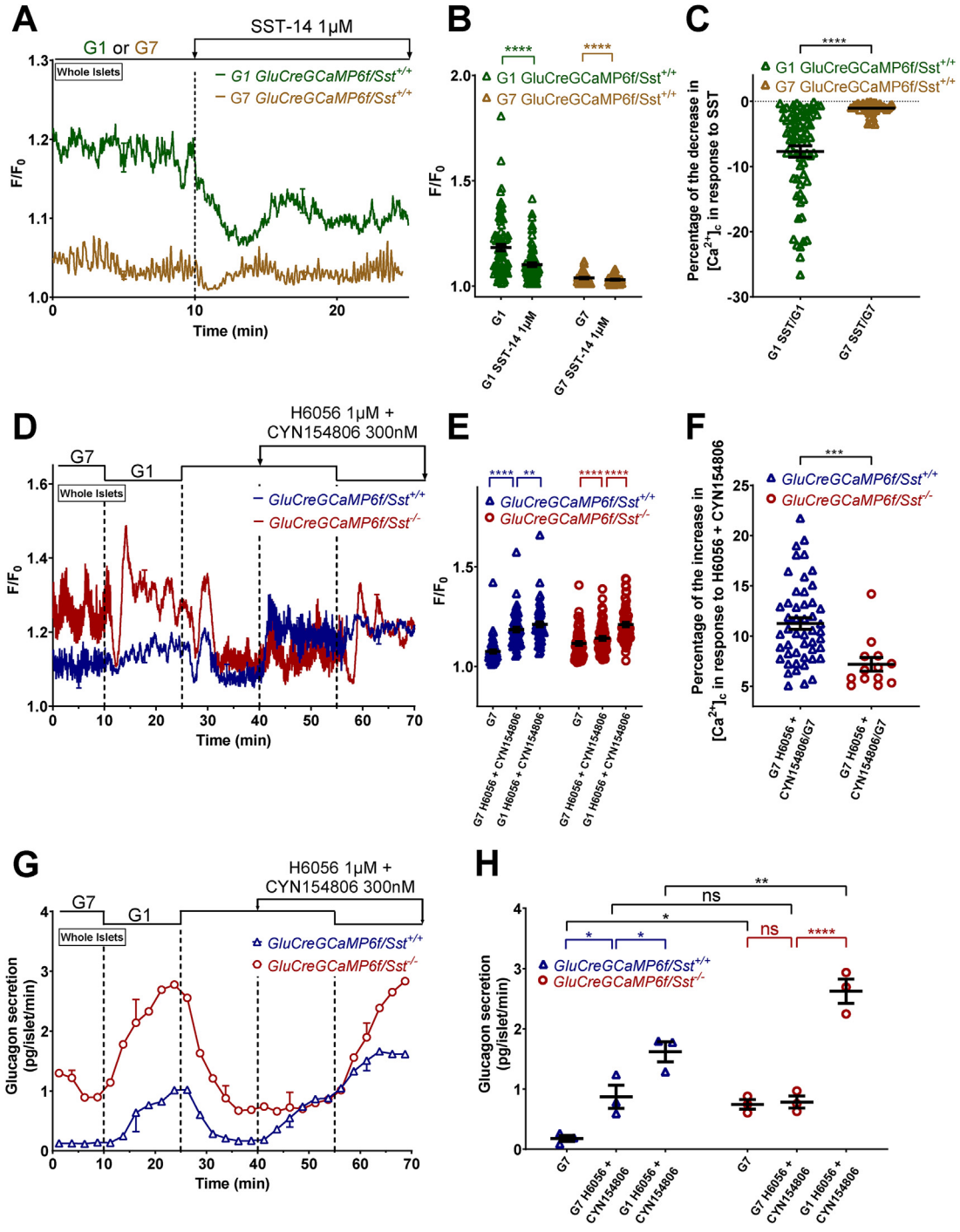


**Figure 2: G1 elevates α-cell $[Ca^{2+}]_c$ and stimulates glucagon secretion by a mechanism that is partly dependent on SST.** α-cell $[Ca^{2+}]_c$ (A–F) and glucagon secretion (G and H) were measured in isolated islets from either *GluCreGCaMP6f/Sst*$^{+/+}$ (brown, green and blue traces) or *GluCreGCaMP6f/Sst*$^{-/-}$ (red traces) mice perifused with 7 mM (G7) and 1 mM glucose (G1). SST-14 (SST-14 1 μM) was added in either G1 or G7 (A–C) whereas H6056 (H6056 1 μM), a SSTR2 and SSTR3 antagonist, was added in combination with CYN154806 (CYN154806 300 nM), a SSTR2 antagonist in G7, when indicated (D–H), to prevent the endogenous action of SST on α-cells. Panels A, D and G represent the mean traces ± SEM from 3 to 5 experiments. Panels B and E represent the scatter plots of individual cells (B, n = 85 cells/11 islets/5 mice for G1 and n = 49 cells/7 islets/3 mice for G7; E, n = 57 cells/5 islets/3 mice for *GluCreGCaMP6f/Sst*$^{+/+}$ and n = 63 cells/7 islets/4 mice for *GluCreGCaMP6f/Sst*$^{-/-}$; one-way RM ANOVA with Sidak correction) with the means ± SEM of the average $[Ca^{2+}]_c$ calculated from panel A (G1 or G7, mean of 2–10 min; G1 SST-14 or G7 SST-14, mean of 17–25 min) and D (G7, mean of 32–40 min; G7 H6056 + CYN15486, mean of 47–55 min, G1 H6056 + CYN154806, mean of 63–70 min), respectively. Panels C and F represent the scatter plot showing the percentage of the decrease or increase in $[Ca^{2+}]_c$ in response to SST-14 (mean of 17–25 min/mean of 2–10 min; two-tailed unpaired t-test) or H6056 + CYN154806 (mean of 47–55 min/mean of 32–40 min; two-tailed unpaired t-test), respectively. Panel H represents the scatter plot of individual experiments with the means ± SEM (Ordinary two-way and two-way RM ANOVA with Sidak correction) of the average glucagon secretion calculated from panel G (G7, mean of 32–40 min; G7 H6056 + CYN15486, mean of 47–55 min, G1 H6056 + CYN154806, mean of 62–70 min). ns, not significant; *P < 0.05; **P < 0.005; ***P < 0.001; ****P < 0.0001.

 

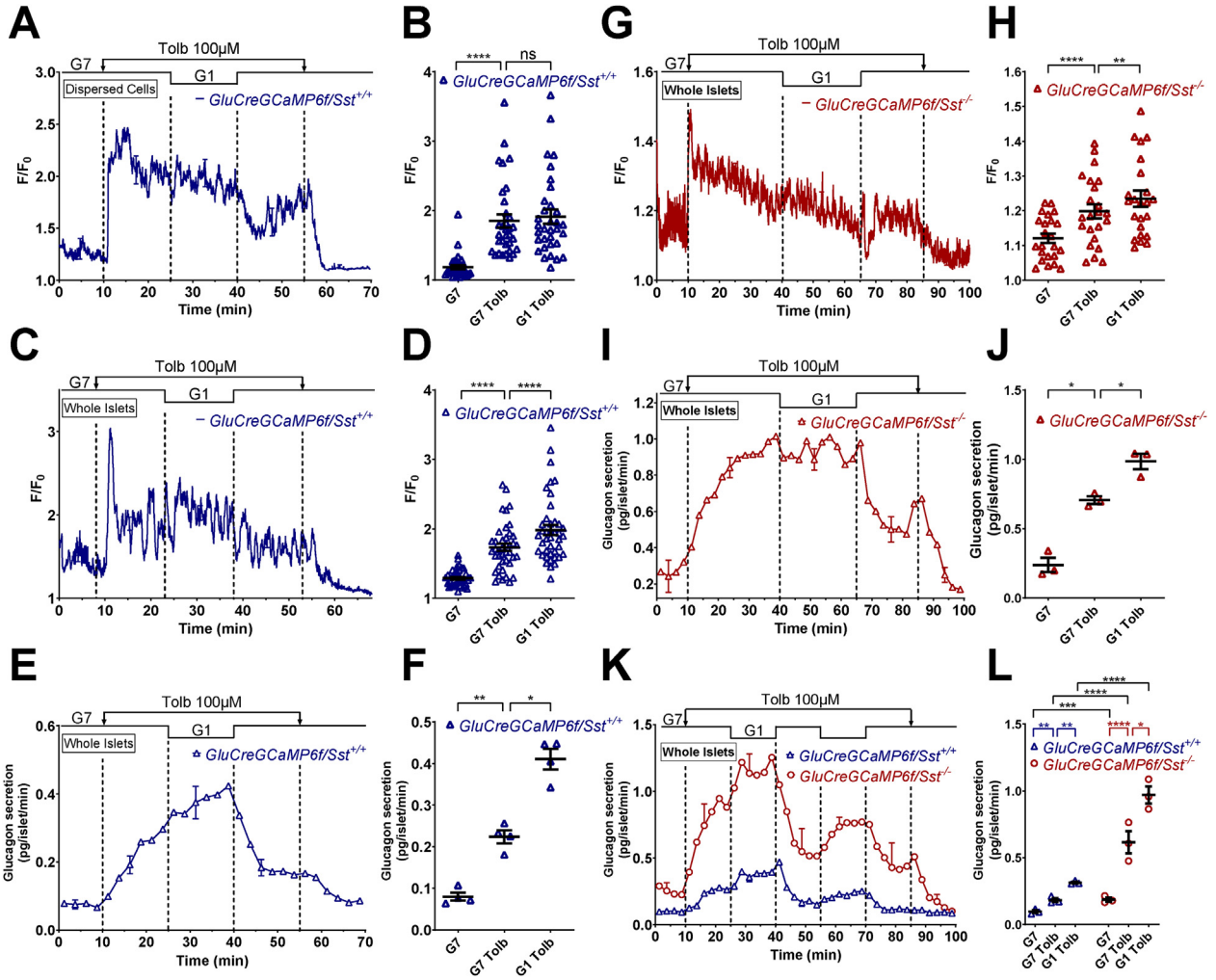


**Figure 3: G1 stimulates glucagon secretion in the presence of tolbutamide.** α-cell $[Ca^{2+}]_c$ was measured in dispersed islet cells (A and B) and isolated islets (C, D, G and H) whereas glucagon secretion was only measured in isolated islets (E, F, I, J, K and L). Dispersed islet cells and isolated islets from *GluCreGCaMP6f/Sst*$^{+/+}$ (blue traces) and isolated islets from *GluCreGCaMP6f/Sst*$^{-/-}$ (red traces) mice were both perifused with 7 mM (G7) and 1 mM glucose (G1). Tolbutamide (Tolb 100 µM), a $K_{ATP}$ channel blocker, was added in G7 as indicated. Panels A, C, E, G I and K represent the mean traces ± SEM of 3–4 experiments. Panels B, D and H represent the scatter plots of individual cells (B, n = 33 cells/3 mice; D, n = 41 cells/4 islets/3 mice; H, n = 34 cells/4 islets/3 mice; one-way RM ANOVA with Sidak correction) with the means ± SEM of the average $[Ca^{2+}]_c$ calculated from panel A (G7, mean of 2–10 min and 62–70 min; G7 Tolb, mean of 17–25 min and 47–55 min; G1 Tolb, mean of 32–40 min), C (G7, mean of 0–8 min and 60–68 min; G7 Tolb, mean of 15–23 min and 45–53; G1 Tolb, mean of 30–38 min) and G (G7, mean of 2–10 min and 92–100 min; G7 Tolb, mean of 32–40 min and 77–85 min; G1 Tolb, mean of 40–48 min), respectively. Panels F, J and L represent the scatter plots of individual experiments with the means ± SEM (F and J, one-way RM ANOVA with Sidak correction; L, Ordinary two-way and two-way RM ANOVA with Sidak correction) of the average glucagon secretion calculated from panel E (G7, mean of 2–10 min and 62–70 min; G7 Tolb, mean of 20–25 min and 50–55 min; G1 Tolb, mean of 36–40 min), I (G7, mean of 2–10 min and 92–100 min; G7 Tolb, mean of 35–40 min and 72–80 min; G1 Tolb, mean of 52–60 min) and K (G7, mean of 2–10 min and 92–100 min; G7 Tolb, mean of 17–25 min, 47–55 min and 77–85 min; G1 Tolb, mean of 32–40 min and 62–70 min), respectively. For panel L, statistics were performed on the logarithm of the values obtained in pg/islet/min from panel K because of the high variability, in accordance with the statistician of our university. ns, not significant; *P < 0.05; **P < 0.005; ***P < 0.001; ****P < 0.0001.

effect on glucagon secretion (Figure 4E,F: blue trace and triangles). Interestingly, in preparations from *GluCreGCaMP6f/Sst*$^{-/-}$ mice, G20 was without effect on $[Ca^{2+}]_c$ in dispersed α-cells (Figure 4A,B: red trace and circles, and Supplementary Figure S5B), whereas it strongly increased $[Ca^{2+}]_c$ in α-cells within islets (Figure 4C,D: red trace and circles, and Supplementary Figure S5D). Mimicking the osmotic effect of G20 by adding 13 mM sucrose, a sugar that is not taken up by GLUT transporters [54], to a medium containing G7 had no effect on $[Ca^{2+}]_c$, ruling out the hypothesis of an osmotic effect (Figure 4A,B, and Supplementary Figure S5A and B). The G20-induced $[Ca^{2+}]_c$ increase in α-cells within *Sst*$^{-/-}$ islets was parallel to a marked increase in glucagon release (Figure 4E,F: red trace and circles). These observations suggest that, in normal islets, a high glucose concentration recruits SST to keep both $[Ca^{2+}]_c$ and glucagon secretion at low levels. This hypothesis is supported by the observation that exogenous SST-14 prevented the rise in α-cell $[Ca^{2+}]_c$ induced by G20 in *GluCreGCaMP6f/Sst*$^{-/-}$ islets (Figure 4G,H).

We next tested whether the glucagonotropic effect of G20 in the absence of SST could be mimicked by an acceleration of glucose metabolism by RO280450, a glucokinase activator. The addition of RO280450 in the presence of G7 did not affect $[Ca^{2+}]_c$ in dispersed α-cells of *GluCreGCaMP6f/Sst*$^{+/+}$ and *GluCreGCaMP6f/Sst*$^{-/-}$ mice

 

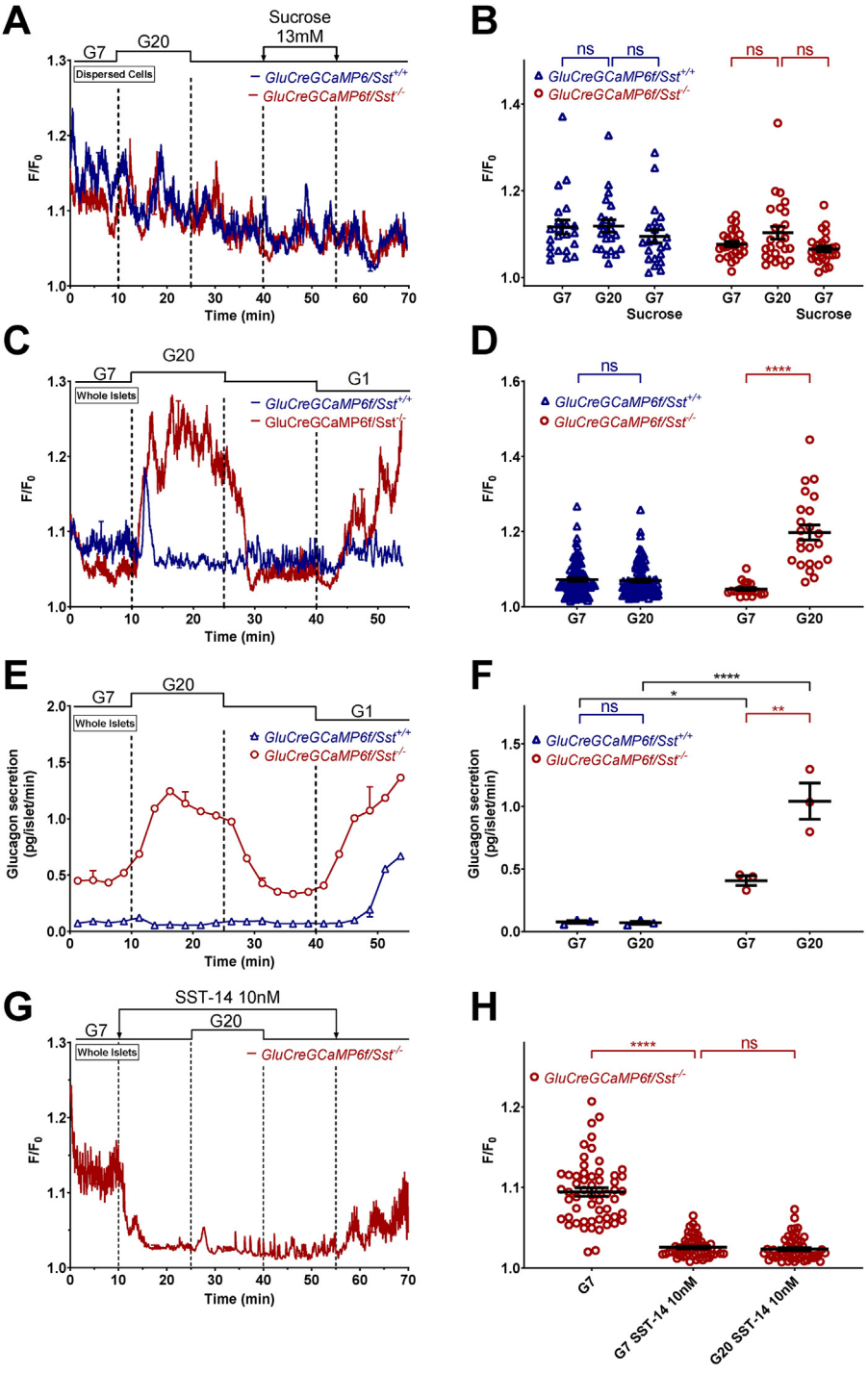


**Figure 4: G20 elevates α-cell $[Ca^{2+}]_c$ and stimulates glucagon secretion in the absence of SST.** α-cell $[Ca^{2+}]_c$ (A-D, G and H) was measured in either dispersed cells (A and B) or whole islets (C, D, G and H) from either *GluCreGCaMP6f/Sst*$^{+/+}$ (blue traces) or *GluCreGCaMP6f/Sst*$^{-/-}$ (red traces) mice. Glucagon secretion was measured in whole islets from either *GluCreGCaMP6f/Sst*$^{+/+}$ (blue trace) or *GluCreGCaMP6f/Sst*$^{-/-}$ (red trace) (E and F). Dispersed cells or whole islets were perifused with 7 mM (G7), 20 mM (G20) and 1 mM glucose (G1). 13 mM sucrose (A and B) was added in G7 as indicated to mimic the osmotic effect of G20 (A and B) whereas SST-14 (SST-14 10 nM) was added in G7 (G and H). Panels A, C, E and G represent the mean traces ± SEM of 3–5 experiments. Panels B, D and H represent the scatter plots of individual cells (B, n = 22 cells/4 mice for *GluCreGCaMP6f/Sst*$^{+/+}$ and n = 26 cells/5 mice for *GluCreGCaMP6f/Sst*$^{-/-}$; D, n = 97 cells/9 islets/5 mice for *GluCreGCaMP6f/Sst*$^{+/+}$ and n = 23 cells/6 islets/3 mice for *GluCreGCaMP6f/Sst*$^{-/-}$; H, n = 57 cells/9 islets/3 mice; one-way RM ANOVA with Sidak correction for B and H, and two-tailed paired t-tests for D) with the means ± SEM of the average $[Ca^{2+}]_c$ calculated from panel A (*GluCreGCaMP6f/Sst*$^{+/+}$: G7, mean of 2–10 min and 25–29 min and 55–59 min; G20, mean of 17–25 min; G7 sucrose, mean of 48–50 min; *GluCreGCaMP6f/Sst*$^{-/-}$: G7, mean of 2–10 min and 32–40 min and 62–70 min; G20, mean of 17–25 min; G7 sucrose, mean of 47–55 min), C (G7, mean of 2–10 min and 32–40 min; G20, mean of 10–25 min) and G (G7, mean of 2–10 min and 62–70 min; G7 SST-14 10 nM, mean of 17–25 min and 47–55 min; G20 SST-14 10 nM, mean of 32–40 min), respectively. Panel F represents the scatter plot of individual experiments with the means ± SEM (Ordinary two-way and two-way RM ANOVA with Sidak correction) of the average glucagon secretion calculated from panel E (G7, mean of 2–10 min and 32–40 min; G20, mean of 10–25 min). ns, not significant; *P < 0.05; **P < 0.005; ****P < 0.0001.

 

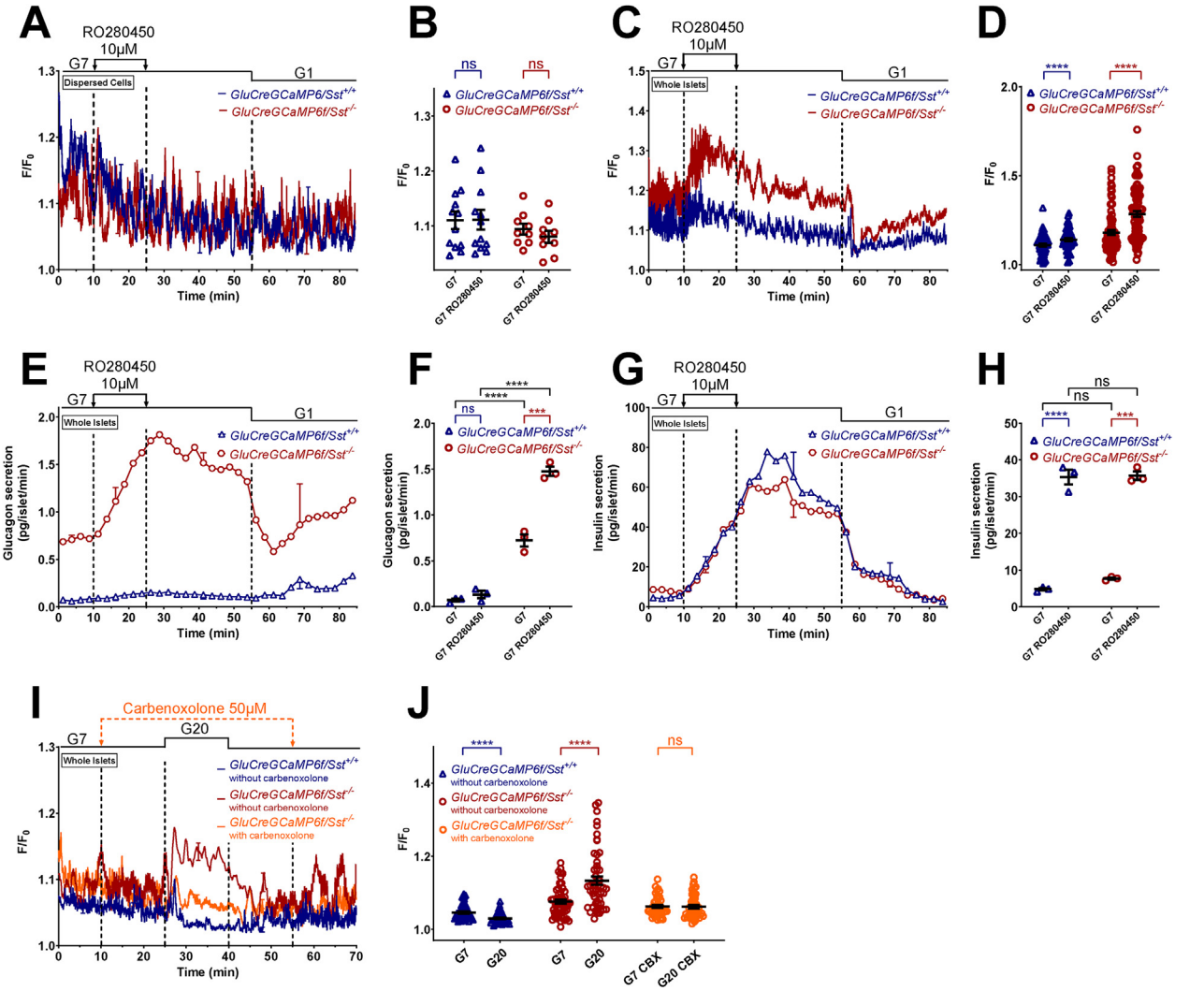


**Figure 5: Stimulating glucose metabolism elevates α-cell $[Ca^{2+}]_c$ and stimulates glucagon secretion in the absence of SST.** α-cell $[Ca^{2+}]_c$ (A-D, I and J) was measured in either dispersed cells (A and B) or whole islets (C, D, I and J) from either *GluCreGCaMP6f/Sst*$^{+/+}$ (blue traces) or *GluCreGCaMP6f/Sst*$^{-/-}$ (red and orange traces) mice. Glucagon (E and F) and insulin secretions (G and H) were measured in whole islets from either *GluCreGCaMP6f/Sst*$^{+/+}$ (blue traces) or *GluCreGCaMP6f/Sst*$^{-/-}$ (red traces). Dispersed cells or whole islets were perifused with 7 mM (G7) and 1 mM glucose (G1). RO280450 (RO280450 10 µM), a glucokinase activator, was added in G7 to mimic the action of a high glucose concentration (G20) (A–H) when indicated. Carbenoxolone (CBX 50 µM) was added in G7 and G20 when indicated and only in one set of experiments with *GluCreGCaMP6f/Sst*$^{-/-}$ (orange trace) (I and J). Panels A, C, E, G and I represent the mean traces ± SEM of 3–5 experiments. Panels B, D and J represent the scatter plots of individual cells (B, n = 12 cells/3 mice for *GluCreGCaMP6f/Sst*$^{+/+}$ and n = 9 cells/3 mice for *GluCreGCaMP6f/Sst*$^{-/-}$; D, n = 56 cells/8 islets/3 mice for *GluCreGCaMP6f/Sst*$^{+/+}$ and n = 80 cells/10 islets/5 mice for *GluCreGCaMP6f/Sst*$^{-/-}$; J, n = 52 cells/8 islets/3 mice for *GluCreGCaMP6f/Sst*$^{+/+}$, n = 53 cells/8 islets/3 mice for *GluCreGCaMP6f/Sst*$^{-/-}$ and n = 47 cells/7 islets/3 mice for *GluCreGCaMP6f/Sst*$^{-/-}$ with carbenoxolone, two-tailed paired t-tests) with the means ± SEM of the average $[Ca^{2+}]_c$ calculated from panel A (*GluCreGCaMP6f/Sst*$^{+/+}$: G7, mean of 2–10 min and 47–55 min; G7 RO280450, mean of 10–23 min; *GluCreGCaMP6f/Sst*$^{-/-}$: G7, mean of 2–10 min and 47–55 min; G7 RO280450, mean of 17–25 min) and C (G7, mean of 2–10 min; G7 RO280450, mean of 17–25 min) and I (G7 or G7 CBX, mean of 17–25 min and 47–55 min; G20 or G20 CBX, mean of 32–40 min), respectively. Panels F and H represent the scatter plots of individual experiments with the means ± SEM (Ordinary two-way and two-way RM ANOVA with Sidak correction) of the average glucagon and insulin secretions calculated from panel E and G (G7, mean of 2–10 min; G7 RO280450, mean of 17–25 min), respectively. ns, not significant; ***P < 0.001; ****P < 0.0001.

(Figure 5A,B, and Supplementary Figure S6A and B). It slightly increased $[Ca^{2+}]_c$ in α-cells from *GluCreGCaMP6f/Sst*$^{+/+}$ islets, but it did not significantly stimulate glucagon secretion (Figure 5C–F: blue traces and triangles, and Supplementary Figure S6C). By contrast, it induced a large increase in $[Ca^{2+}]_c$ in α-cells from *GluCreGCaMP6f/Sst*$^{-/-}$ islets that was associated with a strong stimulation of glucagon release (Figure 5C–F: red traces and circles, and Supplementary Figure S6D). Thus, it recapitulated the effect of G20, except for the slow onset and reversibility of the RO280450 effects. Interestingly, the rate of insulin secretion was similar between *GluCreGCaMP6f/Sst*$^{+/+}$ and *GluCreGCaMP6f/Sst*$^{-/-}$ islets, suggesting that SST does not act as a tonic inhibitor of insulin secretion (Figure 5G,H), as recently reported [29].

Since G20 and RO280450 failed to affect $[Ca^{2+}]_c$ in dispersed α-cells, the sustained $[Ca^{2+}]_c$ increase they induce in α-cells within islets in the absence of endogenous SST could result from a direct action on α-cells that are rendered competent by contacts with neighboring islet cells or by the islet microenvironment. Alternatively, it might involve an indirect control of α-cell activity by acceleration of glucose metabolism, possibly through β-cells. Indeed, the glucokinase activator strongly stimulated

 

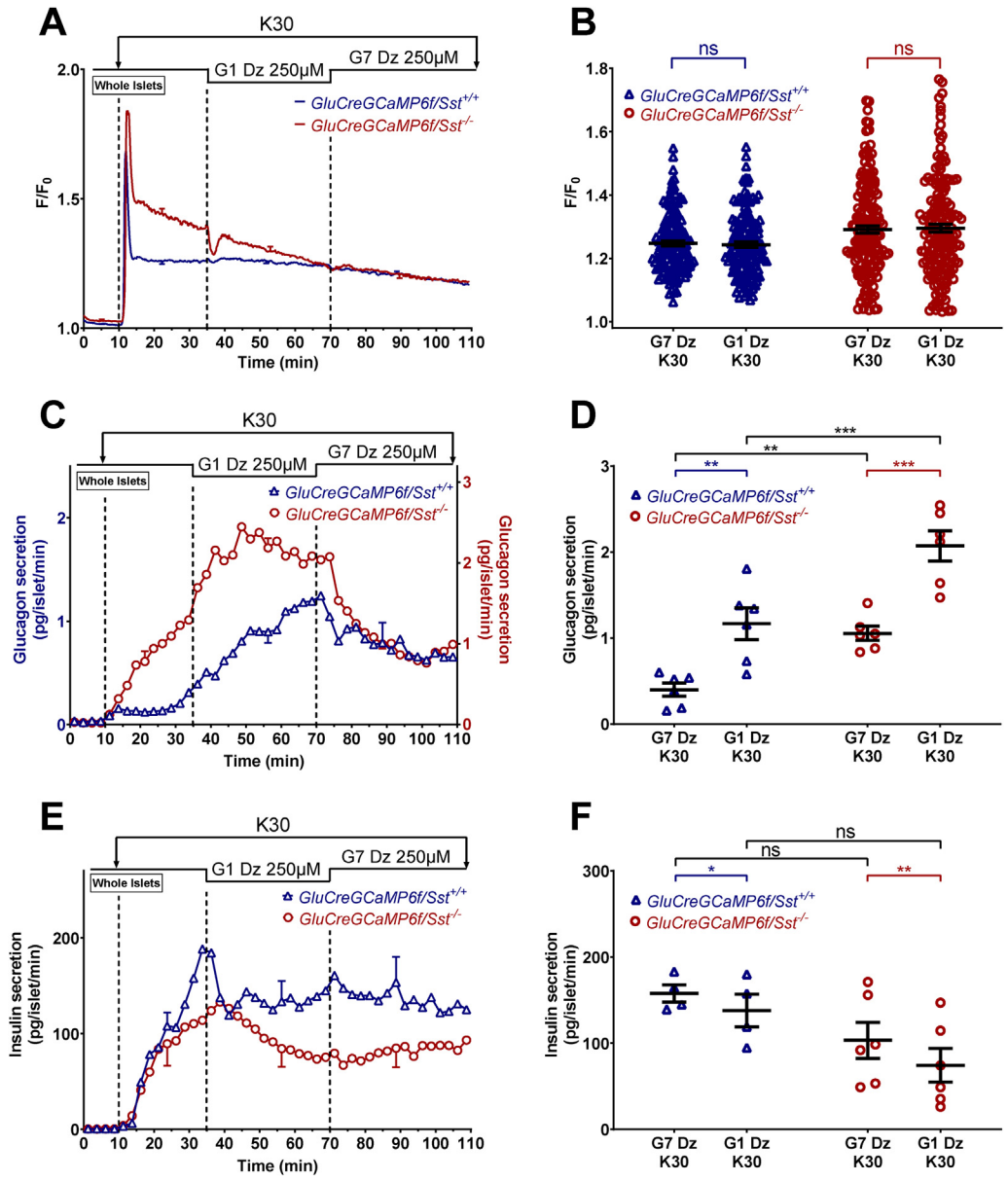


**Figure 6: Low glucose (G1) increases the efficacy of α-cell $[Ca^{2+}]_c$ on glucagon secretion.** α-cell $[Ca^{2+}]_c$ (A and B), glucagon (C and D) and insulin secretions (E and F) were measured in isolated islets from either *GluCreGCaMP6f/Sst*$^{+/+}$ (blue traces) or *GluCreGCaMP6f/Sst*$^{-/-}$ (red traces) mice perifused with 1 mM (G1) and 7 mM glucose (G7) and pretreated with thapsigargin (2 μM) for 2 h. When indicated, the $K^+$ concentration of the medium was increased from 4.8 to 30 mM (K30). Diazoxide (Dz 250 μM), a $K_{ATP}$ channel opener, was present throughout. Panels A, C and E represent the mean traces ± SEM of 6–7 experiments. Panel B represents the scatter plots of individual cells (n = 141 cells/12 islets/6 mice for *GluCreGCaMP6f/Sst*$^{+/+}$ and n = 167 cells/15 islets/7 mice for *GluCreGCaMP6f/Sst*$^{-/-}$, two-tailed paired t-tests) with the means ± SEM of the average $[Ca^{2+}]_c$ calculated from panel A (*GluCreGCaMP6f/Sst*$^{+/+}$: G7 Dz K30, mean of 27–35 min and 70–75 min; G1 Dz K30, mean of 65–70 min; *GluCreGCaMP6f/Sst*$^{-/-}$: G7 Dz K30, mean of 27–35 min and 102–110 min; G1 Dz K30, mean of 50–60 min). Panels D and F represent the scatter plots of individual experiments with the means ± SEM (Ordinary two-way and two-way RM ANOVA with Sidak correction) of the average glucagon and insulin secretions calculated from panel C and E (G7 Dz K30, mean of 27–35 min and 100–105 min; G1 Dz 30, mean of 62–70 min), respectively. ns, not significant; *P < 0.05; **P < 0.005; ***P < 0.001.

insulin secretion of both *GluCreGCaMP6f/Sst*$^{+/+}$ and *GluCreGCaMP6f/Sst*$^{-/-}$ islets. Possible mechanisms of this indirect control involve paracrine factors or electrical coupling. To evaluate this possibility, we tested whether carbenoxolone (CBX), an inhibitor of gap junctions [47,55–57] and of pannexin 1 channels (*Panx1*) [58], altered the effect of G20 on α-cell $[Ca^{2+}]_c$ from *GluCreGCaMP6f/Sst*$^{-/-}$ islets. CBX fully prevented the $[Ca^{2+}]_c$ rise elicited by G20 in SST lacking islets (Figure 5I,J). One potential side-effect of CBX is an inhibition of VGCC [55]. However, this is unlikely the case since the drug did not decrease α-cell $[Ca^{2+}]_c$ during sustained depolarization with high $K^+$ but instead increased it (Supplementary Figure S6E and F). A previous report showed that CBX did not inhibit action potentials in islets [57]. Altogether, these data suggest that, in the absence of SST, glucose-stimulated β-cells entrain α-cells.

 

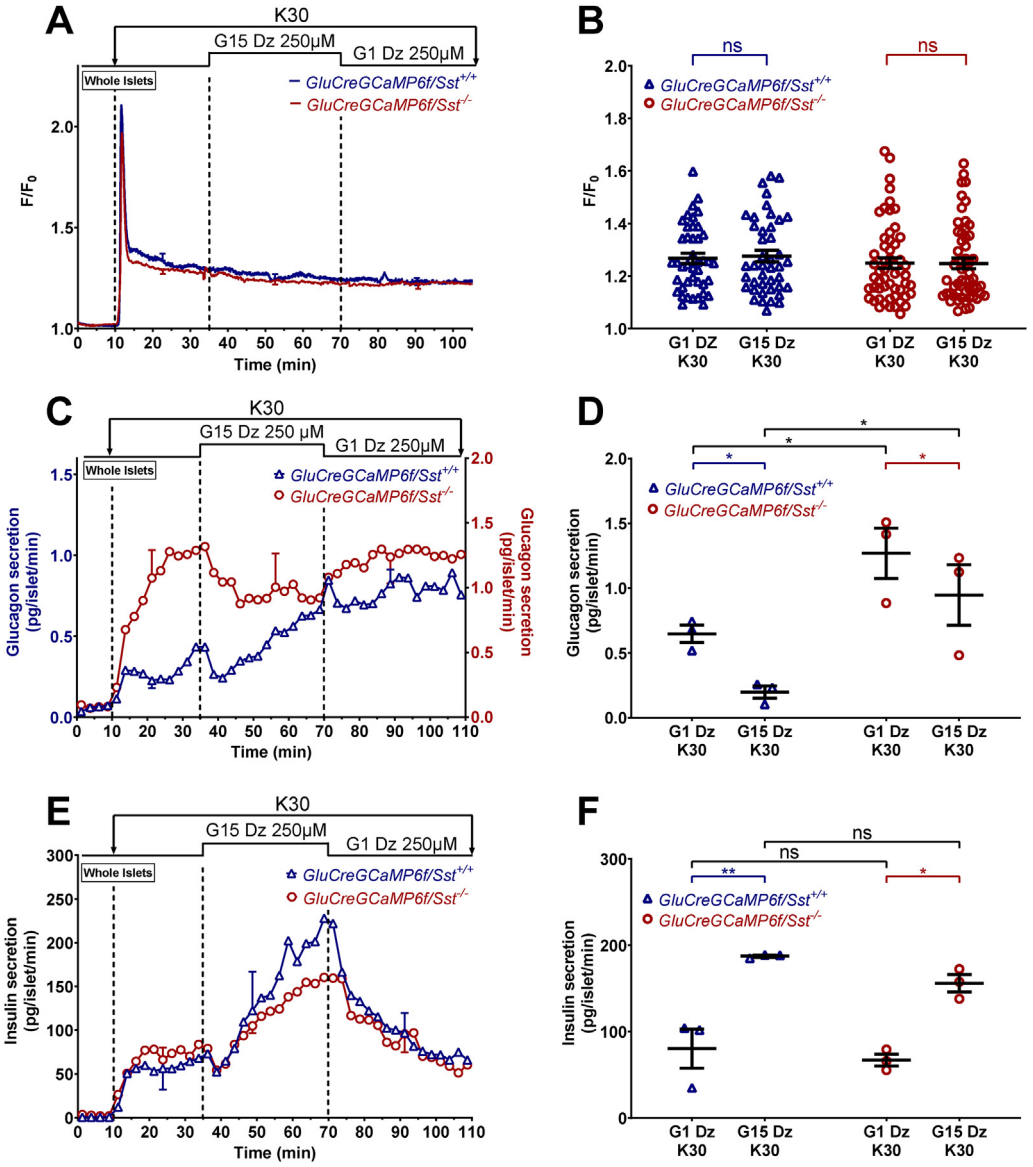


**Figure 7: High glucose (G15) decreases the efficacy of α-cell $[Ca^{2+}]_c$ on glucagon secretion.** α-cell $[Ca^{2+}]_c$ (A and B), glucagon (C and D) and insulin secretions (E and F) were measured in isolated islets from either *GluCreGCaMP6f/Sst*$^{+/+}$ (blue traces) or *GluCreGCaMP6f/Sst*$^{-/-}$ (red traces) mice perifused with 1 mM (G1) and 15 mM glucose (G15) and pretreated with thapsigargin (2 µM) for 2 h. When indicated, the $K^+$ concentration of the medium was increased from 4.8 to 30 mM (K30). Diazoxide (Dz 250 µM), a $K_{ATP}$ channel opener, was present throughout. Panels A, C and E represent the mean traces ± SEM of 3–4 experiments. Panel B represents the scatter plots of individual cells (n = 42 cells/3 islets/3 mice for *GluCreGCaMP6f/Sst*$^{+/+}$ and n = 55 cells/7 islets/4 mice for *GluCreGCaMP6f/Sst*$^{-/-}$, two-tailed paired t-tests) with the means ± SEM of the average $[Ca^{2+}]_c$ calculated from panel A (G1 Dz K30, mean of 30–35 min and 90–95 min; G15 Dz K30, mean of 40–50 min). Panels D and F represent the scatter plots of individual experiments with the means ± SEM (Ordinary two-way and two-way RM ANOVA with Sidak correction) of the average glucagon and insulin secretions calculated from panel C (*GluCreGCaMP6f/Sst*$^{+/+}$: G1 Dz K30, mean of 30–35 min and 85–92 min; G15 Dz K30, mean of 37–45 min; *GluCreGCaMP6f/Sst*$^{-/-}$: G1 Dz K30, mean of 30–35 min and 85–92 min; G15 Dz K30, mean of 42–50 min) and E (G1 Dz K30, mean of 26–35 min and 102–110 min, G15 Dz K30, mean of 62–70 min), respectively. ns, not significant; *P < 0.05; **P < 0.005.

### 3.4. Glucose decreases the efficacy of $Ca^{2+}$ on exocytosis in α-cells by mechanisms that are independent of SST

Several experiments above showed that G1 strongly stimulated glucagon release while it mildly increased α-cell $[Ca^{2+}]_c$. This suggests that the control of glucagon secretion by LG could be partly independent of $[Ca^{2+}]_c$ changes. To assess this hypothesis, we used the experimental procedure that made possible to demonstrate the amplifying pathway of glucose on insulin secretion [59,60]. We applied a high concentration (250 µM) of the $K_{ATP}$ channel opener, diazoxide, to keep $K_{ATP}$ channels open and, thereby, render them insensitive to a change in glucose metabolism. Thereafter, we increased the $K^+$ concentration of the medium to 30 mM $K^+$ (K30) to depolarize α-cells and steadily raise $[Ca^{2+}]_c$. To avoid that any change in $[Ca^{2+}]_c$ involving the ER might affect secretion, islets were pretreated with thapsigargin (2 µM), a specific blocker of SERCA. Increasing the extracellular $K^+$ concentration (K30) strongly increased α-cell $[Ca^{2+}]_c$, but, for unknown reasons, to a larger extent in *GluCreGCaMP6f/Sst*$^{-/-}$ than in *GluCreGCaMP6f/Sst*$^{+/+}$ islets. This $[Ca^{2+}]_c$ rise stimulated glucagon secretion in both types of islets (Figure 6A–D). Switching from G7 to G1 in the presence of K30 and diazoxide did not affect α-

 

cell $[Ca^{2+}]_c$ except for a slight and transient decrease in *GluCreGCaMP6f/Sst*$^{-/-}$ islets. However, it induced a stimulation of glucagon secretion that was attested by a drop of glucagon release upon G7 readmission (Figure 6C,D). A clear stimulatory effect of G1 was also observed in less stringent stimulatory conditions, i.e. in the presence of K20 instead of K30 (Supplementary Figure S7A and B). As expected, switching from G7 to G1 slightly inhibited insulin release (Figure 6E,F).

We next wondered whether the inverse phenomenon could be observed when increasing the glucose concentration from 1 to 15 mM (G15). Switching from G1 to G15 did not affect α-cell $[Ca^{2+}]_c$ in both *GluCreGCaMP6f/Sst*$^{+/+}$ and *GluCreGCaMP6f/Sst*$^{-/-}$ islets (Figure 7A,B), but it induced an inhibition of glucagon release that was transient in *GluCreGCaMP6f/Sst*$^{+/+}$ islets and sustained in *GluCreGCaMP6f/Sst*$^{-/-}$ islets (Figure 7C,D). As expected from the amplifying pathway in β-cells, G15 strongly stimulated insulin release (Figure 7E,F). Interestingly, K30 stimulated glucagon secretion much more in SST-lacking islets than in SST-expressing islets despite the similar α-cell $[Ca^{2+}]_c$ levels in both strains, whereas it stimulated insulin secretion to a similar extent in both types of islets (Figure 7). This again suggests that SST is more effective at inhibiting glucagon than insulin secretion.

Since our previous data showed that increasing glucose concentration from 7 to 20 mM stimulated glucagon secretion of *Sst*$^{-/-}$ islets in conditions where the membrane potential was not clamped (see Figure 4E,F), we wondered whether G20 could also stimulate glucagon release under clamping conditions. We elected to perform these experiments in mildly depolarizing conditions (K20) to avoid that a massive depolarization by K30 masks a stimulatory effect. Switching from G7 to G20 in the presence of diazoxide and K20 only slightly and transiently decreased α-cell $[Ca^{2+}]_c$, but it induced an unexplained transient stimulation of glucagon release that was followed by a sustained inhibition which was more evident in *GluCreGCaMP6f/Sst*$^{-/-}$ than in *GluCreGCaMP6f/Sst*$^{+/+}$ islets (Supplementary Figure S8A-D). These results suggest that G20 does not increase the efficacy of $Ca^{2+}$ on exocytosis.

Overall, these data suggest that an increase of glucose concentration inhibits the efficacy of $Ca^{2+}$ on exocytosis in α-cells in an opposite way to the situation in β-cells and independently of SST.

## 4. DISCUSSION

Using the *GluCreGCaMP6f* mouse model, we evaluated the effect of different glucose concentrations on α-cell $[Ca^{2+}]_c$ and glucagon secretion. Changes in $[Ca^{2+}]_c$ were compared between α-cells within whole islets by confocal microscopy and dispersed α-cells by epifluorescence. Our data indicate that glucose (G7 *versus* G1, or G7 *versus* G20) does not affect $[Ca^{2+}]_c$ in dispersed α-cells. However, the situation is different in α-cells within islets. Indeed, decreasing glucose concentration from 7 to 1 mM increases $[Ca^{2+}]_c$ in some α-cells within islets while it strongly stimulates glucagon secretion from islets. These effects have SST-dependent and -independent components but are independent of α-cell $K_{ATP}$ channels. Interestingly, increasing the glucose concentration from 7 to 20 mM has no effect on α-cell $[Ca^{2+}]_c$ (except for a transient increase) and glucagon secretion in normal islets while it strongly increases both parameters in the absence of paracrine influence of SST. This suggests that, in normal islets, SST released in response to G20 counteracts the stimulatory effect of high glucose on both $[Ca^{2+}]_c$ and glucagon secretion. Our data also show that an elevation of glucose concentration inhibits glucagon secretion independently of α-cell $[Ca^{2+}]_c$, by decreasing the efficacy of $Ca^{2+}$ on exocytosis. These observations highlight the multiple mechanisms of control of glucagon secretion by glucose.

### 4.1. Glucose modulates $[Ca^{2+}]_c$ in α-cells within islets but not in dispersed α-cells

We observed that decreasing glucose concentration from 7 to 1 mM did not significantly affect $[Ca^{2+}]_c$ in dispersed α-cells, in accordance with previous results, including ours, showing subtle to no effect of glucose on $[Ca^{2+}]_c$ in dispersed mouse α-cells [14–16]. Very subtle and variable effects were also observed with 1 mM glucose in α-cells within islets. However, imaging several hundreds of α-cells made possible to reveal that, despite the large intercellular variability, decreasing the glucose concentration produced a statistically significant increase in $[Ca^{2+}]_c$. This is fully consistent with a recent study also performed on a large number of cells [35]. Interestingly, we found that dispersed α-cells were much less active than α-cells within islets, in line with a previous report [9]. The stimulatory effect of sulfonylureas on $[Ca^{2+}]_c$ in dispersed α-cells rules out the possibility of cell dysfunction. Thus, it seems that dispersing α-cells induces a decrease of their $[Ca^{2+}]_c$ oscillatory activity and a loss of responsiveness to G1. The mechanisms responsible for the difference in activity could involve the loss of physical intercellular interactions (including juxtacrine influence and electrical coupling), or paracrine/autocrine factors induced by the dispersion [20]. Decreased $[Ca^{2+}]_c$ activity and responsiveness to glucose also occur in β-cells when isolated [8,61–63].

Increasing glucose concentration from 7 to 20 mM was without effect on $[Ca^{2+}]_c$ of dispersed α-cells of both *Sst*$^{+/+}$ and *Sst*$^{-/-}$ mice whereas it strongly increased that of α-cells from *Sst*$^{-/-}$ islets. Although the reduced activity of dispersed α-cells compared with α-cells within islets might explain this loss of responsiveness, it more likely results from a lack of an indirect signal produced by β-cells. Indeed, we observed that activating β-cell metabolism with glucose or the glucokinase activator RO280450 strongly stimulated insulin secretion. Moreover, while RO280450 increased $[Ca^{2+}]_c$ in α-cells within whole *Sst*$^{-/-}$ islets, it failed to increase $[Ca^{2+}]_c$ in dispersed α-cells.

### 4.2. Glucose-induced changes in α-cell $[Ca^{2+}]_c$ and glucagon secretion are independent of α-cell $K_{ATP}$ channels

The role of $K_{ATP}$ channels in the control of α-cell $[Ca^{2+}]_c$ by glucose is highly debated [7,17,20]. One hypothesis suggests that the drop in α-cell $[Ca^{2+}]_c$ induced by glucose results from a closure of $K_{ATP}$ channels leading to an inactivation of low-threshold voltage-gated channels and a reduction in action potential amplitude and $Ca^{2+}$ influx through VGCC [21–24]. The present study and others do not support this model and showed that closure of $K_{ATP}$ channels by tolbutamide or gliclazide increased, but did not decrease, $[Ca^{2+}]_c$ in α-cells whether they were dispersed or within islets [11,14,25–27,29]. By contrast, we observed that HG (G20, in this study) did not increase $[Ca^{2+}]_c$ of dispersed α-cells, in agreement with the lack of effect of HG on $I_{KATP}$ [14]. Thus, sulfonylureas exert the same effect in α- and β-cells, as outlined in our previous study [29], but glucose exerts a different effect. Our experiments testing the effect of glucose in the presence of $K_{ATP}$ channel inhibitors even support the existence of a $K_{ATP}$ channel-independent control of α-cells by glucose. Indeed, switching from NG (G7) to LG (G1) slightly elevated $[Ca^{2+}]_c$ in the presence of tolbutamide or gliclazide in α-cells within *Sst*$^{-/-}$ and *Sst*$^{+/+}$ islets. This was associated with a stimulation of glucagon release. This is in agreement with previous results showing an inhibition of glucagon release by increasing the glucose concentration in the presence of tolbutamide [11,25] or in the absence of functional $K_{ATP}$ channels in *Sst*$^{-/-}$ and

 

*Sst*$^{+/+}$ islets [28,43]. However, in the absence of sulfonylureas, we do not exclude that $K_{ATP}$ channels of non α-cells indirectly influence glucose-induced changes in α-cell $[Ca^{2+}]_c$ and glucagon secretion. It is important to keep in mind that the lack of effect of glucose on α-cell $K_{ATP}$ channels does not mean that these channels are unnecessary to see the effect of glucose. Indeed, a full opening of these channels by diazoxide decreased α-cell $[Ca^{2+}]_c$ and glucagon release at very low levels and therefore prevented a modulation of glucagon secretion by glucose which requires higher $[Ca^{2+}]_c$ levels [10,14,21,24,26,28,64,65–67].

### 4.3. Glucose-induced changes in α-cell $[Ca^{2+}]_c$ and glucagon secretion involve both SST-dependent and -independent mechanisms

The present study reveals that SST is partly involved in the control of α-cell $[Ca^{2+}]_c$ and that this involvement depends on the glucose concentration, being modest in the LG to NG range and important in the NG to HG range. Indeed, switching from NG (G7) to LG (G1) increased α-cell $[Ca^{2+}]_c$ in both *Sst*$^{-/-}$ and *Sst*$^{+/+}$ islets, and in *Sst*$^{+/+}$ islets perifused with or without SSTR2/3 antagonists, demonstrating that this $[Ca^{2+}]_c$ rise is independent of SST. However, SST probably also contributes to the control of $[Ca^{2+}]_c$ in this range of glucose concentrations because the amplitude of the average increase was lower in α-cells of *Sst*$^{-/-}$ islets than in those of *Sst*$^{+/+}$ islets (see Figure 1E). Moreover, application of SSTR2/3 antagonists in G7 increased $[Ca^{2+}]_c$ much more in α-cells of *Sst*$^{+/+}$ islets than in α-cells of *Sst*$^{-/-}$ islets (Figure 2D,E). This effect likely reflects an alleviation of an inhibition by endogenous SST, the secretion of which is known to be stimulated by G7 [11,17,20,28,44]. We have no explanation for the small increase in $[Ca^{2+}]_c$ in α-cells of *Sst*$^{-/-}$ islets in response to SSTR antagonists. It might reflect a non-specific effect which was however too small to affect glucagon release (Figure 2D,G). The amplitude of the increase in $[Ca^{2+}]_c$ in response to SSTR antagonists was however higher in *Sst*$^{+/+}$ islets than in *Sst*$^{-/-}$ islets (Figure 2F), suggesting that the strong $[Ca^{2+}]_c$ increase in *Sst*$^{+/+}$ islets was not attributed to a non-specific effect of the antagonists. The contribution of SST to the control of α-cell $[Ca^{2+}]_c$ in the NG range is also supported by the observation that exogenous SST induced a larger drop in α-cell $[Ca^{2+}]_c$ when applied at G1 than at G7 (Figure 2A–C), probably because endogenous SST released in response to G7 already decreased $[Ca^{2+}]_c$ and masked most of the effect of exogenously applied SST.

The involvement of SST in the control of α-cell $[Ca^{2+}]_c$ is more important in the higher range of glucose concentration. Thus, switching from NG (G7) to HG (G20) induced a transient $[Ca^{2+}]_c$ increase in α-cells of *Sst*$^{+/+}$ islets, but a pronounced and sustained increase in α-cells of *Sst*$^{-/-}$ islets that is recapitulated by the glucokinase activator RO280450 demonstrating that it involves glucose metabolism. Since glucokinase is highly expressed in mouse α-, β- and δ-cells [68,69], this effect of HG might in theory result from a direct effect of HG on α-cells or an indirect effect mediated by neighbouring cells. Experiments with dispersed cells show that it likely results from an indirect effect because both G20 and RO280450 failed to increase $[Ca^{2+}]_c$ in isolated α-cells. The observations that G20 and RO280450 strongly stimulated insulin release suggests that β-cells might be responsible for this indirect effect. β-cells might indirectly control α-cells via gap junctions [47,56,57] or pannexin 1 channels (*Panx1*) [58] since the G20-induced $[Ca^{2+}]_c$ in α-cells of *Sst*$^{-/-}$ islets was fully prevented by CBX. Connexins are responsible for electrical coupling between adjacent cells. Connexin 36 (*Gjd2*) is the main isoform expressed by islet cells, particularly by β-cells [70]. Pannexin channels are generally thought to not form gap junctions as a result of N-glycosylation [71–73]. However, since they allow the leakage of cytosolic molecules, such as ATP and glutamate [70], they could theoretically allow the release of a paracrine factor from β-cells that entrain α-cells. However, several arguments challenge the possibility that the CBX effect we observed is attributed to inhibition of pannexin 1. The mRNA expression of *Panx1* is far lower than that of *Gjd2* in β-cells [68,69]. Moreover, it was shown that β-cells do not express active pannexin 1 channels [74]. These arguments suggest that the inhibitory effect of CBX on $[Ca^{2+}]_c$ that we observed is instead attributed to an inhibition of gap junctions. Overall, this suggests that HG-induced depolarization of β-cells entrains α-cells by electrical coupling, which increases $[Ca^{2+}]_c$ in α-cells of *Sst*$^{-/-}$ islets. Previous experiments monitoring the transfer of a low molecular fluorescent dye injected in one cell to neighboring islet cells support the existence of a coupling between α- and β-cells [75,76]. In *Sst*$^{+/+}$ islets, HG would also stimulate the release of SST by a direct action on δ-cells or indirectly by electrical entrainment of δ-cells by β-cells [47,56]. SST released in response to HG would counteract the indirect stimulation of α-cells by β-cells and keep α-cell $[Ca^{2+}]_c$ at low level. This is supported by the observation that exogenous SST-14 prevented the rise in $[Ca^{2+}]_c$ induced by G20 in α-cells of *Sst*$^{-/-}$ islets. SST might maintain α-cell $[Ca^{2+}]_c$ at low levels by activating hyperpolarizing G protein-gated inwardly rectifying $K^+$ channels (GIRK) [19,77,78] or other channels [29]. Interestingly, switching from NG (G7) to HG (G20) stimulated glucagon secretion in *Sst*$^{-/-}$ islets, whereas it had no effect in *Sst*$^{+/+}$ islets, suggesting that glucagon release follows $[Ca^{2+}]_c$ changes. However, it is very likely that SST, released in response to HG, not only decreases α-cell $[Ca^{2+}]_c$ but also decreases the efficacy of $Ca^{2+}$ on exocytosis. The existence of such a mechanism is revealed by the much larger secretion induced by K30 (in the presence of diazoxide) in *Sst*$^{-/-}$ than in *Sst*$^{+/+}$ islets, despite a similar change in α-cell $[Ca^{2+}]_c$ (Figure 7A–D). It is fully in agreement with our previous observation that both endogenous and exogenous SST inhibited glucagon secretion without affecting α-cell $[Ca^{2+}]_c$ in the presence of high $K^+$ and diazoxide [29]. This mechanism might involve a calcineurin-dependent depriming of secretory granules [79] or a reduction in levels of cAMP which amplifies $Ca^{2+}$-dependent exocytosis in α-cells [37,42,80–83]. It also likely contributes to the tonic inhibition of glucagon release exerted by endogenous SST.

The mechanisms by which glucose controls α-cell $[Ca^{2+}]_c$ independently of SST and their $K_{ATP}$ channels are unknown and likely involve mechanisms affecting the membrane potential, such as the $Na^+/K^+$ pump, TASK1 or $Ca^{2+}$-activated $K^+$ channels (see introduction).

### 4.4. Glucose controls glucagon secretion by changing $[Ca^{2+}]_c$ and by modulating the efficacy of $Ca^{2+}$ on exocytosis

The experiments performed in conditions where the membrane potential was not clamped show that all $[Ca^{2+}]_c$ changes elicited by glucose in α-cells induce parallel changes in glucagon secretion. Thus, the stimulation of glucagon release from *Sst*$^{+/+}$ or *Sst*$^{-/-}$ islets produced by a drop of glucose concentration from NG to LG, in the presence or absence of $K_{ATP}$ channel blockers or SSTR antagonists, was always accompanied by an increase in $[Ca^{2+}]_c$. Likewise, the stimulation of glucagon release from *Sst*$^{-/-}$ islets produced by an elevation of glucose concentration from NG to HG or by the stimulation of glucokinase by RO280450 was also accompanied by a $[Ca^{2+}]_c$ rise, whereas the failure of HG to stimulate glucagon secretion in *Sst*$^{+/+}$ islets was associated with a low $[Ca^{2+}]_c$.

Several arguments suggest that glucose-induced changes in glucagon secretion are not solely driven by changes in $[Ca^{2+}]_c$ but also by a modulation of the efficacy of $Ca^{2+}$ on exocytosis that is

 

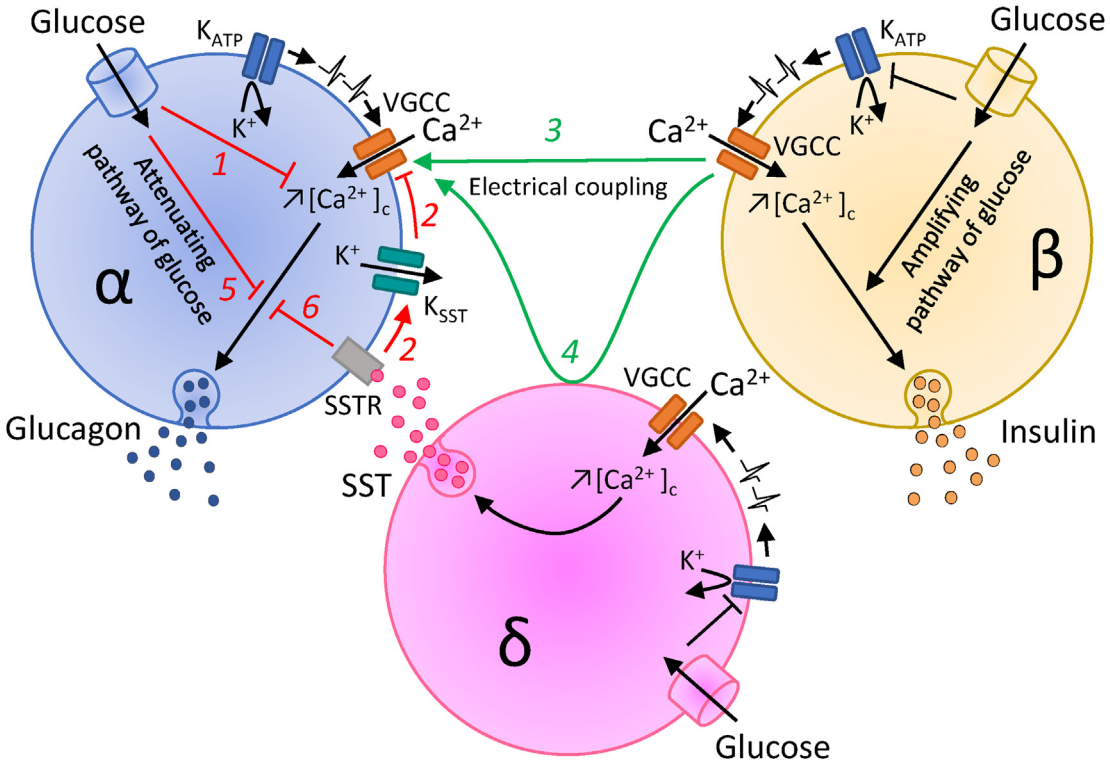


**Figure 8: Model depicting the mechanisms by which glucose controls glucagon release.** Glucose controls glucagon release by multiple mechanisms (inhibitory: red bars; stimulatory: green arrows). Increasing the glucose concentration exerts two opposite effects on α-cell $[Ca^{2+}]_c$. It decreases $[Ca^{2+}]_c$ independently of α-cell $K_{ATP}$ channels (1) and partly via SST (2). It also increases $[Ca^{2+}]_c$ at glucose concentrations that stimulate insulin secretion. This latter effect likely results from electrical coupling which could be direct between β- and α-cells (3), or indirect and involve δ-cells (4). This stimulatory effect on α-cells is counteracted by SST which hyperpolarizes α-cells and keeps α-cell at low levels (2). Hence, it can only be observed in the absence of paracrine influence of SST. All glucose-induced changes in α-cell $[Ca^{2+}]_c$ induce parallel changes in glucagon release. In addition, glucose decreases the efficacy of α-cell $Ca^{2+}$ on exocytosis by an attenuating pathway that is opposite to the amplifying pathway of glucose in β-cells. As previously shown [29], SST released from δ-cells in response to glucose also contributes to the inhibitory effect of glucose by inhibiting the efficacy of $Ca^{2+}$ on exocytosis (6). $K_{ATP}$, ATP-sensitive $K^+$; VGCC, voltage-gated $Ca^{2+}$ channels; SST, somatostatin; SSTR: somatostatin receptor; $K_{SST}$, Hyperpolarizing $K^+$ channel activated by SST (GIRK or another type).

independent of SST. (a) The temporal relationship between changes in $[Ca^{2+}]_c$ and secretion was often poor. Thus, upon switching from NG to LG, $[Ca^{2+}]_c$ quickly reached a plateau whereas glucagon secretion from both *Sst*$^{+/+}$ and *Sst*$^{-/-}$ islets slowly increased. These differences cannot be attributed to differences in the perifusion systems since solution exchange was more rapid for secretion experiments than for $[Ca^{2+}]_c$ imaging. (b) Switching from NG to LG increased $[Ca^{2+}]_c$ in less than half of α-cells within *Sst*$^{+/+}$ islets, and only 1/3 of α-cells within *Sst*$^{-/-}$ islets whereas it strongly stimulated glucagon secretion from both types of islets. (c) Most importantly, experiments performed in conditions where $[Ca^{2+}]_c$ was elevated and the membrane potential was clamped with high $K^+$ and diazoxide showed that LG increased the efficacy of $Ca^{2+}$ on exocytosis, whereas HG exerted the opposite effect. This is opposite to the situation found in β-cells in which the amplifying pathway is activated by an increase in the glucose concentration. The lack of effect of glucose on $[Ca^{2+}]_c$ during prolonged exposure to K30 contrasts with the recently reported glucose inhibition of VGCC in isolated human and mouse α-cells [84]. It is unclear whether these apparently divergent observations are due to the different experimental procedures used and to which extent they reflect similar or distinct phenomena. The glucose-induced decreased efficacy of $Ca^{2+}$ on exocytosis in α-cells was not due to SST since it was also observed and even more pronounced in *Sst*$^{-/-}$ islets. The underlying mechanisms are unknown but cAMP is a good candidate since an increase in glucose concentration induces a $Ca^{2+}$- and SST-independent drop in the cAMP concentration in α-cells that correlates with an inhibition of glucagon release [37,81]. Since insulin can also decrease cAMP in α-cells independently of a change in $[Ca^{2+}]_c$ [42] and since its secretion is stimulated by the amplifying pathway of glucose, it might contribute to the inhibition of glucagon release at HG. However, this is speculative because insulin release was already strongly stimulated by high $K^+$ even at G1, and the HG-induced inhibition of glucagon secretion preceded the stimulation of insulin secretion (Figure 7C,E).

## 5. CONCLUSIONS

Based on our results obtained at different ranges of glucose concentrations, we propose a global model according to which glucose controls α-cell $[Ca^{2+}]_c$ and glucagon secretion through multiple mechanisms that are differentially activated depending on the glucose concentration (Figure 8). At low glucose concentration, small amounts of SST are probably already released and exert a tonic inhibition on glucagon secretion. Increasing glucose concentration above 1 mM slightly decreases $[Ca^{2+}]_c$ in α-cells independently of their $K_{ATP}$ channels and partly via SST. At concentrations that stimulate insulin release (>7 mM) and only in the absence of paracrine influence of SST, glucose increases α-cell $[Ca^{2+}]_c$ probably as a result of their entrainment by electrical

 

coupling via β/α-cells and, possibly also, via β/δ/α-cells. We do not exclude the possibility that this entrainment involves other contact-dependent signaling or stimulatory paracrine factors. However, in normal conditions in which there is a paracrine influence of SST, such increase in α-cell $[Ca^{2+}]_c$ induced by glucose is not seen because SST secreted in response to glucose keeps $[Ca^{2+}]_c$ at low levels (by hyperpolarizing α-cells). Hence, the global effect of an increase of the glucose concentration on α-cell $[Ca^{2+}]_c$ in control conditions is a modest decrease in $[Ca^{2+}]_c$. All α-cell $[Ca^{2+}]_c$ changes induce parallel changes in glucagon secretion, which are however of larger amplitude than those expected from the small $[Ca^{2+}]_c$ fluctuations. The reason is that glucose controls glucagon release by additional mechanisms that are independent of $[Ca^{2+}]_c$ changes. It decreases the efficacy of $Ca^{2+}$ on exocytosis independently of SST (named attenuating pathway in opposition to the amplifying pathway of glucose in β-cells) and also via SST (because glucose stimulates the release of SST which decreases the efficacy of $Ca^{2+}$ on exocytosis [29]). Since $Ca^{2+}$ is required for exocytosis and exerts a permissive role, this inhibitory effect of glucose can only be detected at artificially high $[Ca^{2+}]_c$ (as in the presence of high $K^+$), but it is probably operative already at low $[Ca^{2+}]_c$. Our data suggest that blocking SST paracrine influence would induce hypersecretion of glucagon at high glucose, which is what occurs in diabetes which is characterized by impaired glucagon response to hyperglycemia due to impaired SST secretion [6].

## AUTHORS' CONTRIBUTIONS

P.G. conceived, supervised the study and designed experiments. B.S. designed and performed experiments and analyzed results. F.K. performed experiments and analyzed results. B.S. and P.G. wrote the manuscript. All coauthors approved the manuscript. P.G. and B.S. are guarantors of this work and, as such, have full access to all the data in the study and take responsibility for the integrity of the data and the accuracy of the data analysis.

## FUNDING

This study was supported by a grant from the Actions de Recherche Concertées (18/23—094) from the Communauté française de Belgique, by a Research Credit grant (J.0178.17) and Research Project Grants (T.0124.15 and T.0110.20) from the Fonds National de la Recherche Scientifique (Brussels), by a grant from the Société Francophone du Diabète (Paris), by a grant 1912-03555 from the Leona M. & Harry B. Helmsley Charitable Trust and by a Diatype grant from Innoviris (Brussels). P.G. is Research Director of the Fonds National de la Recherche Scientifique, (Brussels). B.S. was partly supported by a fellowship from UCLouvain, Belgium. F.K. is holder of a fellowship from the FRIA/FNRS, Brussels, Belgium.

## PRIOR PRESENTATION

Parts of this study were presented at the 55th EASD annual meeting, Barcelona, Spain, September 16—20, 2019 and at the SFD annual meeting, Brussels, Belgium, September 8—11, 2020.

## ACKNOWLEDGEMENTS

We thank F. Knockaert and N. Antoine for help for radioimmunoassays and genotyping, respectively, P Herrera (Geneva) for providing *GluCre* mice and E. Gatineau for helpful comments. This work benefited from statistical advices from UCLouvain's technological platform for Methodology and Statistical Computing Support - SMCS/LIDAM, UCLouvain.

## CONFLICT OF INTEREST

None declared.

## APPENDIX A. SUPPLEMENTARY DATA

Supplementary data to this article can be found online at https://doi.org/10.1016/j.molmet.2022.101495.

## REFERENCES

[1] Müller, T.D., Finan, B., Clemmensen, C., Dimarchi, R.D., Tschöp, M.H., 2017. The new biology and pharmacology of glucagon. Physiological Reviews 97(2):721—766.
[2] Holst, J.J., Albrechtsen, N.J.W., Pedersen, J., Knop, F.K., 2017. Glucagon and amino acids are linked in a mutual feedback cycle: the liver-alpha-cell axis. Diabetes 66(2):235—240.
[3] Albrechtsen, N.J.W., Pedersen, J., Galsgaard, K.D., Winther-sørensen, M., Suppli, M.P., Janah, L., et al., 2019. The liver-alpha-cell axis and type 2 diabetes. Endocrine Reviews 40(5):1353—1366.
[4] Rorsman, P., Ashcroft, F.M., 2018. Pancreatic β-cell electrical activity and insulin secretion: of mice and men. Physiological Reviews 98(1):117—214.
[5] Gromada, J., Chabosseau, P., Rutter, G.A., 2018. The α-cell in diabetes mellitus. Nature Reviews Endocrinology 14(12):694—704.
[6] Omar-Hmeadi, M., Lund, P.E., Gandasi, N.R., Tengholm, A., Barg, S., 2020. Paracrine control of α-cell glucagon exocytosis is compromised in human type-2 diabetes. Nature Communications 11(1):1—11.
[7] Gilon, P., 2020. The role of α-cells in islet function and glucose homeostasis in health and type 2 diabetes. Journal of Molecular Biology 432(5):1367—1394.
[8] Gilon, P., Chae, H., Rutter, G.A., Ravier, M.A., 2014. Calcium signaling in pancreatic β-cells in health and in type 2 diabetes. Cell Calcium 56(5):340—361.
[9] Barg, S., Galvanovskis, J., Göpel, S.O., Rorsman, P., Eliasson, L., 2000. Tight coupling between electrical activity and exocytosis in mouse glucagon-secreting A-cells. Diabetes 49:1500—1510.
[10] Liu, Y., Vieira, E., Gylfe, E., 2004. A store-operated mechanism determines the activity of the electrically excitable glucagon-secreting pancreatic α-cell. Cell Calcium 35(4):357—365.
[11] Vieira, E., Salehi, A., Gylfe, E., 2007. Glucose inhibits glucagon secretion by a direct effect on mouse pancreatic alpha cells. Diabetologia 50(2):370—379.
[12] Berts, A., Ball, A., Gylfe, E., Hellman, B., 1996. Suppression of $Ca^{2+}$ oscillations in glucagon-producing $\alpha_2$-cells by insulin/glucose and amino acids. Biochimica et Biophysica Acta 1310(2):212—216.
[13] Olsen, H.L., Theander, S., Bokvist, K., Buschard, K., Wollheim, C.B., Gromada, J., 2005. Glucose stimulates glucagon release in single rat α-cells by mechanisms that mirror the stimulus-secretion coupling in β-cells. Endocrinology 146(11):4861—4870.
[14] Quoix, N., Cheng-xue, R., Mattart, L., Zeinoun, Z., Guiot, Y., Beauvois, C., 2009. Glucose and pharmacological modulators of ATP-sensitive $K^+$ channels control $[Ca^{2+}]_c$ by different mechanisms in isolated mouse α-cells. Diabetes 58(2):412—421.
[15] Rorsman, P., Braun, M., Zhang, Q., 2012. Regulation of calcium in pancreatic α- and β-cells in health and disease. Cell Calcium 51(3—4):300—308.
[16] Le Marchand, S.J., Piston, D.W., 2010. Glucose suppression of glucagon secretion: metabolic and calcium responses from α-cells in intact mouse pancreatic islets. Journal of Biological Chemistry 285(19):14389—14398.

 

[17] Gylfe, E., Gilon, P., 2013. Glucose regulation of glucagon secretion. Diabetes Research and Clinical Practice 103(1):1—10.

[18] Gilon, P., Cheng-xue, R., Lai, B.K., Chae, H., Gomez-Ruiz, A., 2015. Physiological and pathophysiological control of glucagon secretion by pancreatic α-cells. In: Islam, M.S. (Ed.), Islets of Langerhans, 2nd ed. Dordrecht: Springer Science+Business Media. p. 175—247.

[19] Briant, L., Salehi, A., Vergari, E., Zhang, Q., Rorsman, P., 2016. Glucagon secretion from pancreatic α-cells. Upsala Journal of Medical Sciences 121(2): 113—119.

[20] Gylfe, E., 2016. Glucose control of glucagon secretion —'There's a brand-new gimmick every year'. Upsala Journal of Medical Sciences 121(April): 120—132.

[21] Gromada, J., Ma, X., Høy, M., Bokvist, K., Salehi, A., Berggren, P., et al., 2004. ATP-sensitive $K^+$ channel-dependent regulation of glucagon release and electrical activity by glucose in wild-type and $SUR1^{-/-}$ mouse α-cells. Diabetes 53(Suppl. 3):181—189.

[22] Zhang, Q., Dou, H., Rorsman, P., 2020. 'Resistance is futile?' — paradoxical inhibitory effects of $K_{ATP}$ channel closure in glucagon-secreting α-cells. Journal of Physiology 598(21):4765—4780.

[23] Macdonald, P.E., Marinis, YZ De, Ramracheya, R., Salehi, A., Ma, X., Johnson, P.R.V., et al., 2007. A $K_{ATP}$ channel-dependent pathway within α cells regulates glucagon release from both rodent and human islets of Langerhans. PLoS Biology 5(6):e143.

[24] Zhang, Q., Ramracheya, R., Lahmann, C., Tarasov, A., Bengtsson, M., Braha, O., et al., 2013. Role of $K_{ATP}$ channels in glucose-regulated glucagon secretion and impaired counterregulation in type 2 diabetes. Cell Metabolism 18(6):871—882.

[25] Le Marchand, S.J., Piston, D.W., 2012. Glucose decouples intracellular $Ca^{2+}$ activity from glucagon secretion in mouse pancreatic islet alpha-cells. PLoS One 7(10):e47084.

[26] Quoix, N., Cheng-xue, R., Guiot, Y., Herrera, P.L., Henquin, J., Gilon, P., 2007. The GluCre-ROSA26EYFP mouse: a new model for easy identification of living pancreatic α-cells. FEBS Letters 581(22):4235—4240.

[27] Früh, E., Elgert, C., Eggert, F., Scherneck, S., Rustenbeck, I., 2021. Glucagonotropic and glucagonostatic effects of $K_{ATP}$ channel closure and potassium depolarization. Endocrinol (United States). 162(1):1—13.

[28] Cheng-xue, R., Gómez-ruiz, A., Antoine, N., Noël, L.A., Chae, H., Ravier, M.A., et al., 2013. Tolbutamide controls glucagon release from mouse islets differently than glucose. Diabetes 62(5):1612—1622.

[29] Singh, B., Khattab, F., Chae, H., Desmet, L., Herrera, P.L., Gilon, P., 2021. $K_{ATP}$ channel blockers control glucagon secretion by distinct mechanisms: a direct stimulation of α-cells involving a $[Ca^{2+}]_c$ rise and an indirect inhibition mediated by somatostatin. Molecular Metabolism 53:101268.

[30] Bode, H.-P., Weber, S., Fehmann, H.-C., Göke, B., 1999. A nutrient-regulated cytosolic calcium oscillator in endocrine pancreatic glucagon-secreting cells. Pflügers Archiv 437(3):324—334.

[31] Dadi, P.K., Luo, B., Vierra, N.C., Jacobson, D.A., 2015. TASK-1 potassium channels limit pancreatic α-cell calcium influx and glucagon secretion. Molecular Endocrinology 29(5):777—787.

[32] Dickerson, X.M.T., Dadi, P.K., Altman, M.K., Verlage, K.R., Thorson, A.S., Jordan, X.K.L., et al., 2019. Glucose-mediated inhibition of calcium-activated potassium channels limits alpha-cell calcium influx and glucagon secretion. Am J Physiol Endocinol Metab 316(4):E646—E659.

[33] Nadal, A., Quesada, I., Soria, B., 1999. Homologous and heterologous asynchronicity between identified α-, β- and δ-cells within intact islets of Langerhans in the mouse. Journal of Physiology 517(1):85—93.

[34] Quesada, I., Todorova, M.G., Alonso-magdalena, P., Beltra, M., Carneiro, E.M., Martin, F., et al., 2006. Glucose induces opposite intracellular $Ca^{2+}$ concentration oscillatory patterns in identified α- and β-cells within intact human islets of Langerhans. Diabetes 55:2463—2469.

[35] Kellard, J.A., Rorsman, N.J.G., Hill, T.G., Armour, S.L., van de Bunt, M., Rorsman, P., et al., 2020. Reduced somatostatin signalling leads to hypersecretion of glucagon in mice fed a high-fat diet. Molecular Metabolism 40:101021.

[36] Lavagnino, Z., Dwight, J., Ustione, A., Nguyen, T.U., Tkaczyk, T.S., Piston, D.W., 2016. Snapshot hyperspectral light-sheet imaging of signal transduction in live pancreatic islets. Biophysical Journal 111(2):409—417.

[37] Yu, Q., Shuai, H., Ahooghalandari, P., Gylfe, E., Tengholm, A., 2019. Glucose controls glucagon secretion by directly modulating cAMP in alpha cells. Diabetologia 62(7):1212—1224.

[38] Li, J., Yu, Q., Ahooghalandari, P., Gribble, F.M., Reimann, F., Tengholm, A., et al., 2015. Submembrane ATP and $Ca^{2+}$ kinetics in alpha-cells : unexpected signaling for glucagon secretion. The FASEB Journal 29(8):3379—3388.

[39] Asada, N., Shibuya, I., Iwanaga, T., Niwa, K., Kanno, T., 1998. Identification of α- and β-cells in intact isolated islets of Langerhans by their characteristic cytoplasmic $Ca^{2+}$ concentration dynamics and immunocytochemical staining. Diabetes 47(5):751—757.

[40] Hughes, J.W., Ustione, A., Lavagnino, Z., Piston, D.W., 2018. Regulation of islet glucagon secretion: beyond calcium. Diabetes, Obesity and Metabolism 20(suppl. May):127—136.

[41] Hauge-evans, A.C., King, A.J., Carmignac, D., Richardson, C.C., Robinson, I.C.A.F., Low, M.J., et al., 2009. Somatostatin secreted by islet δ-cells fulfills multiple roles as a paracrine regulator of islet function. Diabetes 58(2):403—411.

[42] Elliott, A.D., Ustione, A., Piston, D.W., 2015. Somatostatin and insulin mediate glucose-inhibited glucagon secretion in the pancreatic α-cell by lowering cAMP. Am J Physiol Endocinol Metab 308(2):E130—E143.

[43] Lai, B., Chae, H., Gómez-ruiz, A., Cheng, P., Gallo, P., Antoine, N., et al., 2018. Somatostatin is only partly required for the glucagonostatic effect of glucose but is necessary for the glucagonostatic effect of $K_{ATP}$ channel blockers. Diabetes 67(11):2239—2253.

[44] Xu, S., Andersen, D., Izarzugaza, J., Kuhre, R., Holst, J., 2020. In the rat pancreas, somatostatin tonically inhibits glucagon secretion and is required for glucose-induced inhibition of glucagon secretion. Acta Physiologica 229(3): e13464.

[45] Reissaus, C.A., Piston, D.W., 2017. Reestablishment of glucose inhibition of glucagon secretion in small pseudoislets. Diabetes 66(4):960—969.

[46] Hutchens, T., Piston, D.W., 2015. EphA4 receptor forward signaling inhibits glucagon secretion from α-cells. Diabetes 64(11):3839—3851.

[47] Miranda, C., Begum, M., Vergari, E., Briant, L.J.B., 2022. Gap junction coupling and islet delta-cell function in health and disease. Peptides, 170704.

[48] Ye, L., Haroon, M.A., Salinas, A., Paukert, M., 2017. Comparison of GCaMP3 and GCaMP6f for studying astrocyte $Ca^{2+}$ dynamics in the awake mouse brain. PLoS One 12(7):1—17.

[49] Madisen, L., Garner, A.R., Shimaoka, D., Chuong, A.S., Klapoetke, N.C., Li, L., et al., 2015. Transgenic mice for intersectional targeting of neural sensors and effectors with high specificity and performance. Neuron 85(5):942—958.

[50] Chen, T., Wardill, T.J., Sun, Y., Pulver, S.R., Renninger, S.L., Baohan, A., et al., 2013. Ultrasensitive fluorescent proteins for imaging neuronal activity. Nature 499(7458):295—300.

[51] Herrera, P.L., 2000. Adult insulin- and glucagon-producing cells differentiate from two independent cell lineages. Development 127(11):2317—2322.

[52] Low, M.J., Patel, Y.C., Rubinstein, M., Low, M.J., Otero-corchon, V., Parlow, A.F., et al., 2001. Somatostatin is required for masculinization of growth hormone-regulated hepatic gene expression but not of somatic growth. The Journal of Clinical Investigation 107(12):1571—1580.

[53] Seino, S., Sugawara, K., Yokoi, N., Takahashi, H., 2017. β-Cell signalling and insulin secretagogues: a path for improved diabetes therapy. Diabetes, Obesity and Metabolism 19(Suppl 1):22—29.

[54] Augustin, R., 2010. The protein family of glucose transport facilitators: it's not only about glucose after all. IUBMB Life 62(5):315—333.


 

[55] Manjarrez-Marmolejo, J., Franco-Pérez, J., 2016. Gap junction blockers: an overview of their effects on induced seizures in animal models. Current Neuropharmacology 14(7):759–771.
[56] Briant, L.J.B., Reinbothe, T.M., Spiliotis, I., Miranda, C., Rodriguez, B., Rorsman, P., 2018. δ- and β-cells are electrically coupled and regulate α-cell activity via somatostatin. Journal of Physiology 596(2):197–215.
[57] Lebreton, F., Pirog, A., Belouah, I., Bosco, D., Berney, T., Meda, P., et al., 2015. Slow potentials encode intercellular coupling and insulin demand in pancreatic beta cells. Diabetologia 58(6):1291–1299.
[58] Michalski, K., Kawate, T., 2016. Carbenoxolone inhibits Pannexin1 channels through interactions in the first extracellular loop. The Journal of General Physiology 147(2):165–174.
[59] Henquin, J., 2000. Triggering and amplifying pathways of regulation of insulin secretion by glucose. Diabetes 49(11):1751–1760.
[60] Henquin, J., 2011. The dual control of insulin secretion by glucose involves triggering and amplifying pathways in β-cells. Diabetes Research and Clinical Practice 93(Suppl 1):S27–S31.
[61] Halban, P.A., Wollheim, C.B., Blondel, B., Meda, P., Niesor, E.N., Mintzj, D.H., 1982. The possible importance of contact between pancreatic islet cells for the control of insulin release. Endocrinology 111(1):86–94.
[62] Rkp, Benninger, Head, W.S., Zhang, M., Satin, L.S., Piston, D.W., 2011. Gap junctions and other mechanisms of cell-cell communication regulate basal insulin secretion in the pancreatic islet. Journal of Physiology 589(Pt 22): 5453–5466.
[63] Jonkers, F.C., Jonas, J.C., Gilon, P., Henquin, J.C., 1999. Influence of cell number on the characteristics and synchrony of $Ca^{2+}$ oscillations in clusters of mouse pancreatic islet cells. Journal of Physiology 520(3):839–849.
[64] Quesada, I., Nadal, A., Soria, B., 1999. Different effects of tolbutamide and diazoxide in α-, β-, and δ-cells within intact islets of Langerhans. Diabetes 48(12):2390–2397.
[65] Ramracheya, R., Ward, C., Shigeto, M., Walker, J.N., Amisten, S., Zhang, Q., et al., 2010. Membrane potential-dependent inactivation of voltage-gated ion channels in α-cells inhibits glucagon secretion from human islets. Diabetes 59(9):2198–2208.
[66] Vieira, E., Liu, Y., Gylfe, E., 2004. Involvement of $\alpha_1$ and β-adrenoceptors in adrenaline stimulation of the glucagon-secreting mouse α-cell. Naunyn-Schmiedeberg's Archives of Pharmacology 369(2):179–183.
[67] Hamilton, A., Zhang, Q., Salehi, A., Willems, M., Knudsen, J.G., Ringgaard, A.K., et al., 2018. Adrenaline stimulates glucagon secretion by tpc2-dependent $Ca^{2+}$ mobilization from acidic stores in pancreatic α-cells. Diabetes 67(March):1128–1139.
[68] Adriaenssens, A.E., Svendsen, B., Lam, B.Y.H., Yeo, G.S.H., Holst, J.J., Reimann, F., et al., 2016. Transcriptomic profiling of pancreatic alpha, beta and delta cell populations identifies delta cells as a principal target for ghrelin in mouse islets. Diabetologia 59(10):2156–2165.
[69] Digruccio, M.R., Mawla, A.M., Donaldson, C.J., Noguchi, G.M., Vaughan, J., Cowing-zitron, C., et al., 2016. Comprehensive alpha, beta and delta cell transcriptomes reveal that ghrelin selectively activates delta cells and promotes somatostatin release from pancreatic islets. Molecular Metabolism 5(7):449–458.
[70] Cigliola, V., Allagnat, F., Berchtold, L.A., Lamprianou, S., Haefliger, J.A., Meda, P., 2015. Role of connexins and pannexins in the pancreas. Pancreas 44(8):1234–1244.
[71] Sosinsky, G.E., Boassa, D., Dermietzel, R., Duffy, H.S., Laird, D.W., MacVicar, B.A., et al., 2011. Pannexin channels are not gap junction hemichannels. Channels 5(3):37–41.
[72] Beckmann, A., Grissmer, A., Krause, E., Tschernig, T., Meier, C., 2016. Pannexin-1 channels show distinct morphology and no gap junction characteristics in mammalian cells. Cell and Tissue Research 363(3):751–763.
[73] Ruan, Z., Orozco, I.J., Du, J., Lü, W., 2020. Structures of human pannexin 1 reveal ion pathways and mechanism of gating. Nature 584(7822):646–651.
[74] Scemes, E., Bavamian, S., Charollais, A., Spray, D.C., Meda, P., 2008. Lack of "hemichannel" activity in insulin-producing cells. Cell Communication and Adhesion 15(1–2):143–154.
[75] Michaels, R.L., Sheridan, J.D., 1981. Islets of Langerhans: dye coupling among immunocytochemically distinct cell types. Science 214(4522):801–803, 80.
[76] Meda, P., Kohen, E., Kohen, C., Rabinovitch, A., Orci, L., 1982. Direct communication of homologous and heterologous endocrine islet cells in culture. The Journal of Cell Biology 92(1):221–226.
[77] Yoshimoto, Y., Fukuyama, Y., Horio, Y., Inanobe, A., Gotoh, M., Kurachi, Y., 1999. Somatostatin induces hyperpolarization in pancreatic islet α cells by activating a G protein-gated $K^+$ channel. FEBS Letters 444(2–3):265–269.
[78] Kailey, B., Van De, Bunt M., Cheley, S., Johnson, P.R., Macdonald, P.E., Gloyn, A.L., et al., 2012. SSTR2 is the functionally dominant somatostatin receptor in human pancreatic β- and α-cells. Am J Physiol Endocinol Metab 303(9):E1107–E1116.
[79] Gromada, J., Høy, M., Buschard, K., Salehi, A., Rorsman, P., 2001. Somatostatin inhibits exocytosis in rat pancreatic α-cells by $G_{i2}$-dependent activation of calcineurin and depriming of secretory granules. Journal of Physiology 535(2):519–532.
[80] Gromada, J., Bokvist, K., Ding, W.G., Barg, S., Buschard, K., Renström, E., et al., 1997. Adrenaline stimulates glucagon secretion in pancreatic A-cells by increasing the $Ca^{2+}$ current and the number of granules close to the L-type $Ca^{2+}$ channels. The Journal of General Physiology 110(3):217–228.
[81] Tengholm, A., Gylfe, E., 2017. cAMP signalling in insulin and glucagon secretion. Diabetes, Obesity and Metabolism 19(Suppl 1):42–53.
[82] Tian, G., Sandler, S., Gylfe, E., Tengholm, A., 2011. Glucose- and hormone-induced cAMP oscillations in α- and β-cells within intact pancreatic islets. Diabetes 60(5):1535–1543.
[83] Schuit, F.C., Derde, M.-P., Pipeleers, D.G., 1989. Sensitivity of rat pancreatic A and B cells to somatostatin. Diabetologia 32(3):207–212.
[84] Dai, X.Q., Camunas-Soler, J., Briant, L.J.B., dos Santos, T., Spigelman, A.F., Walker, E.M., et al., 2022. Heterogenous impairment of α cell function in type 2 diabetes is linked to cell maturation state. Cell Metabolism 34(2): 256–268 e5.

 